



# Suppressing the virulence factors of *Candida auris* with baicalein through multifaceted mechanisms

Can Li<sup>1,2</sup> · Jun Wang<sup>4</sup> · Hao Li<sup>1,2</sup> · Yemei Wang<sup>1,2</sup> · Hui Wu<sup>1,2</sup> · Wenfan Wei<sup>1,2</sup> · Daqiang Wu<sup>1,2</sup> · Jing Shao<sup>1,2</sup> · Tianming Wang<sup>1,2</sup> · Changzhong Wang<sup>1,2,3</sup>

Received: 15 May 2024 / Revised: 1 June 2024 / Accepted: 8 June 2024 / Published online: 11 July 2024  
© The Author(s), under exclusive licence to Springer-Verlag GmbH Germany, part of Springer Nature 2024

## Abstract

*Candida auris*, a rapidly spreading multi-drug-resistant fungus, is causing lethal infections under certain conditions globally. Baicalin (BE), an active ingredient extracted from the dried root of *Scutellaria baicalensis* Georgi, exhibits antifungal activity. However, studies have shown the distinctive advantages of Traditional Chinese medicine in combating fungal infections, while the effect of BE, an active ingredient extracted from the dried roots of *Scutellaria baicalensis* Georgi, on *C. auris*, remains unknown. Therefore, this study aims to evaluate the potential of BE as an antifungal agent against the emerging multidrug-resistant *C. auris*. Various assays and models, including microbroth dilution, time growth curve analysis, spot assays, adhesion tests, flocculation test, cell surface hydrophobicity assay, hydrolase activity assays, XTT assay, violet crystal assay, scanning electron microscope (SEM), confocal laser scanning microscope (CLSM), flow cytometry, Live/dead fluorescent staining, reactive oxygen species (ROS), cell wall assay, aggregation assay, porcine skin model, *Galleria mellonella* larvae (*G. mellonella* larvae) infection model, and reverse transcription–quantitative polymerase chain reaction (RT-PCR) were utilized to investigate how baicalein suppresses *C. auris* through possible multifaceted mechanisms. The findings indicate that BE strongly inhibited *C. auris* growth, adhesion, and biofilm formation. It also effectively reduced drug resistance and aggregation by disrupting the cell membrane and cell wall while reducing colonization and invasion of the host. Transcriptome analysis showed significant modulation in gene expression related to different virulence factors post-BE treatment. In conclusion, BE exhibits significant effectiveness against *C. auris*, suggesting its potential as a viable treatment option due to its multifaceted suppression mechanisms.

---

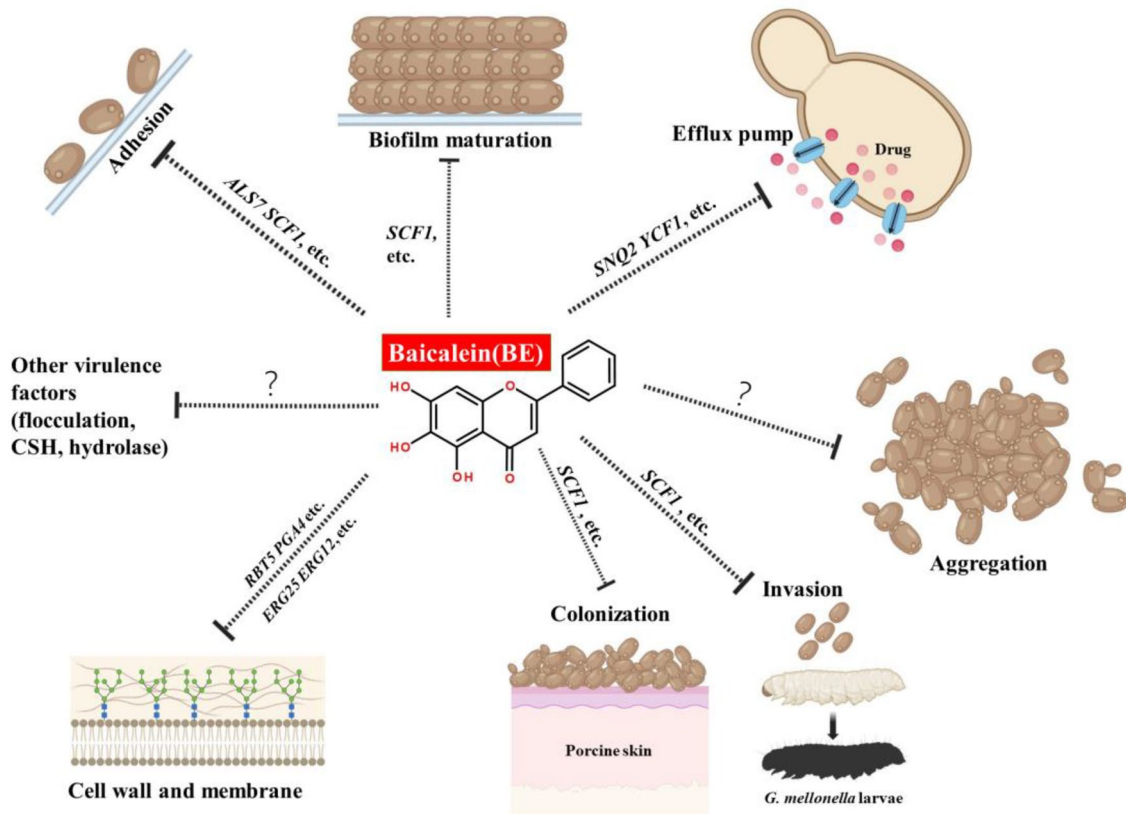
Communicated by Yusuf Akhter.

✉ Changzhong Wang  
ahwcz63@sina.com

- <sup>1</sup> Department of Pathogenic Biology and Immunology, College of Integrated Chinese and Western Medicine (College of Life Science), Anhui University of Chinese Medicine, Hefei, China
- <sup>2</sup> Institute of Integrated Traditional Chinese and Western Medicine, Anhui University of Chinese Medicine, Hefei, China
- <sup>3</sup> Anhui Province Key Laboratory of Chinese Medicinal Formula, Anhui University of Chinese Medicine, Hefei, China
- <sup>4</sup> Anhui Provincial Institute for Food and Drug Control, Hefei, China

### Graphical abstract

Schematic representation of this study. Baicalein (BE) can effectively hinder the growth and colonization of *C. auris* by disrupting the expression of multiple virulence factors. This results in a strong antifungal effect, providing protection to the host from infection.



**Keywords** *Candida auris* · Baicalein · Virulence · Biofilm

### Abbreviations

ABC	ATP-binding cassette	FLZ	Fluconazole
ALS	Agglutinin-like sequence	<i>G. mellonella larvae</i>	<i>Galleria mellonella larvae</i>
BE	Baicalein	GPI	Glycosylphosphatidylinositol
BSA	Bovine serum albumin	HaCaT	Human Keratinocytes Cells
<i>C. auris</i>	<i>Candida auris</i>	HZ	Zone of hemolytic activity
<i>C. albicans</i>	<i>Candida albicans</i>	LD 50	Median lethal dose
CFW	Calcofluor white	MFC	Minimum fungicidal concentration
CLSM	Confocal laser scanning microscope	MIC	Minimum inhibitory concentration
COVID-19	Corona Virus Disease 2019	OD	Optical Density
CSH	Cell surface hydrophobicity	PBS	Phosphate buffered saline
DCFH-DA	2',7'-Dichlorodihydrofluorescein diacetate	PCA	Principal Component Analysis
DMEM	Dulbecco's modified Eagle's medium	PI	Propidium iodide
FBS	Fetal Bovine Serum	PZ	Zone of precipitation
FDA	Fluorescein Diacetate	ROS	Reactive oxygen species
		RPMI-1640	Roswell Park Memorial Institute-1640
		Rt-qPCR	Reverse transcription–quantitative polymerase chain reaction

SEM	Scanning electron microscope
SMIC	Sessile minimum inhibitory concentration
XTT	2, 3-Bis (2-methoxy-4-nitro-5-sulfophenyl)-5-[(phenylamino) carbonyl]-2H-tetrazolium hydroxide
YPD	Yeast Peptone Dextrose

## Introduction

*Candida auris*, initially identified in Japan in 2009, has become a widespread multidrug-resistant fungus known as a 'superbug' (Satoh et al. 2009). It has emerged as a global epidemic, leading to outbreaks of nosocomial infections with high mortality rates and rising levels of antifungal resistance (Ahmad et al. 2020). Over the past decade, *C. auris* infections have increased in over 40 countries and territories across six continents (Du et al. 2020), exhibiting genetic diversity across five distinct evolutionary clades (Chow et al. 2019). The COVID-19 pandemic has also facilitated the spread of *C. auris* (Ben Abid et al. 2023). In recent years, traditional antifungal drugs, including azoles, polyenes, and echinocandins, have been mainly used in clinical settings. The emergence of multidrug-resistant *C. auris* indicates its resistance to several standard antifungal drugs, including fluconazole, amphotericin B, and caspofungin. This situation also underscores the limitations of these drugs, including their high toxicity, significant drug interactions, and increased costs for specific formulations (Vélez et al. 2024). A significant challenge exists in treating fungal infectious diseases, emphasizing the need for new drugs and innovative approaches to treat notorious fungal infections.

Baicalein (BE) is a predominant constituent found in *Scutellaria baicalensis*, it exhibits various pharmacological effects, such as antioxidant, anti-inflammatory, antibacterial, antineoplastic, and antiviral properties (Yan et al. 2020). Additionally, it does not exhibit toxicity toward normal cells, including blood and liver cells (Wu et al. 2018). Its primary application is in treating acute and chronic inflammatory diseases (Li-Weber 2009). *Candida albicans* is a vital member of the *Candida* family. Previous research has shown that BE (0.023–370.1  $\mu\text{M}$ ) exhibits an inhibitory effect on *C. albicans*, resulting in reduced overall growth, biofilm formation, metabolic activity, and cell surface hydrophobicity. This effect is dosage-dependent (Shirley et al. 2017). Other research has suggested the combination of BE and quercetin effectively reduces biofilm formation and mycelial growth of *Candida albicans*, while also increasing cell membrane permeability. RT-qPCR results indicate that the combination of BE and quercetin significantly enhances the expression of hypha-related genes (*ALS3*, *HYR1*, and *CPHI*) compared to

BE or quercetin alone. Thus, the potential efficacy of combining BE and quercetin as anti-*Candida* agents has been proven. (Janeczko et al. 2022). BE treatment could also induce apoptosis in *C. albicans* cells by disrupting mitochondrial membrane potential. The study revealed a significant increase in intracellular ROS levels after processing with BE, as compared to untreated cells, accompanied by elevated expression of *CAP1* (a key regulatory gene of oxidative stress response), *SOD2* (manganese superoxide dismutase gene) and *TRR1* (thioredoxin reductase gene). (Dai et al. 2009). In conclusion, these studies have shown that BE is effective as an antifungal agent and suggest its potential use as a solution for *C. auris* biofilm-related infections.

However, studies have shown the distinctive advantages of Traditional Chinese medicine in combating fungal infections, while the effect of baicalein (BE), an active ingredient extracted from the dried roots of *Scutellaria baicalensis* Georgi on *C. auris*, remains unknown. Therefore, this study aims to evaluate the potential of BE as an antifungal agent against the emerging multidrug-resistant *C. auris* by inhibiting adhesion, biofilm formation, and its detrimental effects on the cell membrane and cell wall. The findings from this study could significantly contribute to expanding therapeutic options for fungal infectious diseases, and it may hold substantial theoretical and research value.

## Material and methods

### *Candida auris* strains and cultivation

*C. auris* strains (C1, C2, C3, and C4) were provided by Prof. Huang Guanghua from FuDan University. *C. auris* was cultured on Yeast Peptone Dextrose (YPD) Agar, then activated in YPD Broth (Hopebio Biotechnology Co., Ltd, Shandong, China) and incubated at 37 °C for 12–14 h until the exponential phase. The fungal precipitate was obtained through centrifuging at 825  $\times$  g for 5 min, and the supernatant was discarded. Roswell Park Memorial Institute -1640 (RPMI-1640) medium (Thermo Fisher, New York, USA; pH 7.0) was then added to adjust the concentration to  $2 \times 10^3$ ,  $1 \times 10^6$ ,  $2 \times 10^6$ ,  $7 \times 10^6$ ,  $1 \times 10^7$ ,  $2 \times 10^7$ , and  $2 \times 10^8$  CFU/ml.

### MIC

The minimum inhibitory concentration (MIC) of the drugs against the four *C. auris* strains was determined following the broth microdilution method in 96-well plates following the CLSI M27-M44S protocol guidelines of the American Committee for Standardization of Clinical Trials. The fungal suspension was adjusted to a concentration of  $2 \times 10^3$  cells/ml. Drugs were then prepared in serial two-fold dilution,

with BE (CAS 491–67-8, HPLC  $\geq$  98%, Shanghai Yuanye Biotechnology Co., Ltd) ranging from 0.23–1894.6  $\mu$ M and FLZ (CAS 86,386–73–4, Shanghai Yuanye Biotechnology Co., Ltd) ranging from 209–3343.5  $\mu$ M. Subsequently, 100  $\mu$ l of the fungal suspension and 100  $\mu$ l of the drug solution were added to each well. The well plates were incubated at 37 °C for 24 h. The MIC of the drug against *Candida* was determined by visually observing sterile growth (Zhang et al. 2024).

### MFC

The minimum fungicidal concentration (MFC) of BE was carried out for four *C. auris* strains. The fungal suspension was adjusted to a concentration of  $2 \times 10^3$  cells/ml. Drugs were then prepared in serial two-fold dilution, with BE ranging from 0.23–1894.6  $\mu$ M and FLZ ranging from 209–3343.5  $\mu$ M. Subsequently, 100  $\mu$ l of the fungal suspension and 100  $\mu$ l of the drug solution were added to each well. The well plates were incubated at 37 °C for 24 h. After incubation, the four wells were chosen before and after MIC values, and from all the wells, the 100  $\mu$ l samples were transferred into YPD Agar medium. After 24 h incubation, the plates and existence of colonies were observed and the absence of colonies were noted as minimum fungicidal concentration and results were noted (Nandhagopal et al. 2024).

### Spot assay

The *C. auris* cells were grown overnight in liquid YPD media at 37°C. They were exposed to varying concentrations of BE or FLZ at densities of  $2 \times 10^5$ ,  $2 \times 10^4$ ,  $2 \times 10^3$  and  $2 \times 10^2$  CFU/ml. After serially diluting cultures (5  $\mu$ l), we spotted them on YPD agar plates. Growth differences were observed after 24 h of incubation at 37°C (Zhang et al. 2024).

### Time growth curve

During the logarithmic growth phase, the concentration of *C. auris* was adjusted to  $2 \times 10^6$  cells/ml. Subsequently, 7.4, 14.8, 29.6, and 59.2  $\mu$ M of BE and 209  $\mu$ M of FLZ were added to the *C. auris* suspension. Additionally, a control group without drugs was established. After incubation for 0, 6, 12, 18, and 24 h, the cells were collected through centrifugation at  $825 \times g$  for 5 min. They were diluted with phosphate buffered saline (PBS) and spread onto the YPD agar medium. After 48 h of incubation at 37 °C, the colonies were counted as CFU/ml (Wei et al. 2024).

### Transcriptome sequencing

Total RNA for transcriptome sequencing was extracted from *C. auris* in the control ( $n = 3$ ) and BE (59.2  $\mu$ M)

( $n = 3$ ) groups. The concentration, purity, and integrity of the extracted RNA underwent assessment using a Nanodrop2000 system and agarose gel electrophoresis. After A-T base pairing with poly-A using magnetic beads with oligo (d-T), mRNA was isolated from the total RNA. This mRNA was then added to a fragmentation buffer to isolate a small fragment of approximately 300 bp, which was subsequently reverse-transcribed into cDNA. The adaptor was ligated after the formation of a stable double-stranded structure. Sequencing was conducted using the Illumina NovaSeq 6000 sequencing platform. Genes with a threshold of  $|\log_2\text{FC}| > 1$  and a  $p$ -value  $< 0.05$  were selected for further analysis. Gene set cluster analysis, sample relationship analysis, and expression difference analysis were employed to interpret the gene expression data (Wu et al. 2024).

### Flocculation test

The concentration of *C. auris* during the logarithmic growth phase was adjusted to  $2 \times 10^6$  cells/ml. Subsequently, 7.4, 14.8, 29.6, and 59.2  $\mu$ M of BE and 209  $\mu$ M of FLZ were added to the suspension of *C. auris*. Additionally, a control group that received no treatment was also included. The suspension was incubated at 37 °C in a constant temperature box for 24 h. After incubation, the tubes were vigorously oscillated for a few seconds, then 100  $\mu$ l of the liquid from the bottom of the test tube was aspirated into a clean 96-well plate using a micropipette (Gelis et al. 2012). The liquid was examined under a DMi8 microscope (Leica, Wetzlar, Hesse, Germany) at  $200 \times$  magnification.

### Cell surface hydrophobicity

The cell surface hydrophobicity (CSH) of *C. auris* was measured using the two-phase water-hydrocarbon. A suspension of *C. auris* ( $2 \times 10^6$  cells/ml) was added to a 6-well plate, together with concentrations of 7.4, 14.8, 29.6, and 59.2  $\mu$ M of BE and 209  $\mu$ M of FLZ. A control group without treatment was included. After biofilm formation, we removed the supernatant and resuspended the cells in sterile PBS. After centrifugation at  $825 \times g$  for 5 min, we removed the supernatant and resuspended the precipitate in PBS. The concentration was then adjusted to an  $\text{OD}_{600}$  of 1.0. We collected 1.2 mL of the fungal suspension from each group and added 0.3 mL of *n*-octane (Shanghai Aladdin Bio-Chem Technology Co., Ltd, China). After vortexing, we let the suspension stand for approximately 15 min to separate the two phases. The lower liquid phase was collected with a pipette and examined at a wavelength of 600 nm. After removing the aqueous phase, we measured the optical density (OD) value at 600 nm. The  $\text{OD}_{600}$  value of PBS without octane served as the blank control, and CSH was calculated



as  $(OD_{600 \text{ control}} - OD_{600 \text{ experiment}}) / OD_{600 \text{ control}}$  (Zhang et al. 2024).

## Adhesion

The slides, each with a 1 cm<sup>2</sup> surface area, were soaked in a 75% ethanol solution for 24 h. Following that, they were rinsed with sterile PBS. A suspension of *C. auris* at a concentration of  $2 \times 10^6$  cells/ml was added to a 6-well plate, along with different concentrations of BE (7.4, 14.8, 29.6, 59.2  $\mu$ M) and FLZ (209  $\mu$ M). The plates were subsequently incubated at 37 °C for 2 and 4 h (Zhang et al. 2015). Following this, the slides were stained in the dark for 30 min using a newly configured fluorescein diacetate (FDA, 10  $\mu$ M, Sparkjade Biotechnology Co., Ltd., Shandong, China). The cells were observed and photographed using a DMi8 microscope (Leica, Wetzlar, Hesse, Germany) at 400 $\times$  magnification.

In each well of a six-well plate, 2 mL of Human keratinocyte cells (HaCaT) at a concentration of  $2 \times 10^5$  cells/ml were added and allowed to culture for 24 h at 37 °C in an environment containing 5% CO<sub>2</sub>. Following this, a *C. auris* suspension at a concentration of  $2 \times 10^7$  cells/ml was added to the six-well plate (Hu et al. 2023), along with varying concentrations of BE (7.4, 14.8, 29.6, 59.2  $\mu$ M) and FLZ (209  $\mu$ M). The plate was incubated in an incubator at 37 °C with 5% CO<sub>2</sub> for 6 h. After that, the specimens were rinsed 2–3 times with sterile PBS and treated with 4% paraformaldehyde at room temperature for 15 min. Excess liquid was then shaken off, and the cells were washed again with sterile PBS before being stained using an enhanced Gram staining kit. The adherence of *C. auris* was observed under a DMi8 microscope (Leica, Wetzlar, Hesse, Germany) at 200 $\times$  magnification.

## Proteinase activity

In a medium containing bovine serum albumin (BSA), 0.05% MgSO<sub>4</sub>, 2% glucose, 0.1% KH<sub>2</sub>PO<sub>4</sub>, 1% BSA, and 2% agar, 10  $\mu$ l of a prepared fungal suspension ( $1 \times 10^6$  cells/ml) was mixed with equal quantities of drugs (7.4, 14.8, 29.6, 59.2  $\mu$ M BE, and 209  $\mu$ M FLZ). This mixture was then added dropwise onto the surface of the BSA medium. The mixture was then incubated at 37°C for 3–4 days (Kumar et al. 2015). The control group did not receive any drugs. We analyzed the effect of the drugs on proteinase activity based on the PZ value, which was calculated as the colony diameter divided by the sum of the precipitation circle and the colony diameters. A PZ value of 1.0 indicated no proteinase activity, and no precipitation circle was observed around the colony. A PZ value less than 1.0 indicated a precipitation circle around the colony, with a larger circle indicating higher proteinase activity of *C. auris*.

## Phospholipase activity

A fungal suspension ( $1 \times 10^6$  cells/ml) was mixed with equal drug quantities (7.4, 14.8, 29.6, 59.2  $\mu$ M BE, and 209  $\mu$ M FLZ) in egg yolk agar base containing 10% (v/v) sterile egg yolk emulsion (Hopebio Biotechnology Co., Ltd, Shandong, China). This mixture was then added dropwise onto the surface of the egg yolk medium and incubated at 37°C for 2–4 days (Kumar et al. 2015; Larkin et al. 2017). The PZ value was determined using the method employed for proteinase activity.

## Esterase activity

In the lipase medium (1% peptone, 0.055% CaCl<sub>2</sub>, 5% NaCl, 1.5% agar, and 0.5% Tween-80, 10  $\mu$ l of a prepared fungal suspension ( $1 \times 10^6$  cells/ml) was mixed with equal drug quantities (7.4, 14.8, 29.6, 59.2  $\mu$ M BE, and 209  $\mu$ M FLZ) using a micropipette. The mixture was then added dropwise onto the surface of the BSA medium and incubated for 3–4 days at 37°C (Oyardi et al. 2023). A control group without drugs was included. We evaluated the effect of BE on esterase secretion based on the PZ value, which was calculated using the same method as for proteinase activity analysis.

## Hemolytic activity

On the Columbia CNA Blood Agar Plate (HuanKai Microbial Biotechnology Co., Ltd, Guangdong, China), we combined 10  $\mu$ l of a prepared fungal suspension ( $1 \times 10^6$  cells/

**Table 1** Primers sequences used for RT-qPCR

Gene	Primer sequences
<i>C. auris- ACT1</i>	Forward (5'-3'): GTCGGTGATGAGGCTCAATCCAAG Reverse (5'-3'): GTCGTCCCAGTTCGTGACAATACC
<i>C. auris- RBT5</i>	Forward (5'-3'): TTCCAAGCCAGAAACCACCTCTAC Reverse (5'-3'): AGCAGACGCAGCAGCAGAAG
<i>C. auris- PGA4</i>	Forward (5'-3'): TGCTAGAGACGATGGTGCTAACTG Reverse (5'-3'): CACGAACAACCTGCCTTCACTTGG
<i>C. auris- ERG12</i>	Forward (5'-3'): CGTACTCCATTAAGATCGAGT Reverse (5'-3'): CTGATTTGGTGGGTGGCGTAGC
<i>C. auris- ERG25</i>	Forward (5'-3'): CATCGCATCGTAGGCATCCATAGC Reverse (5'-3'): GCAACAAGGAGCAGTGGGAGTG
<i>C. auris- SNQ2</i>	Forward (5'-3'): GCTGGTGCCACTGCCTCAAC Reverse (5'-3'): TGGGAAACACGCTTCTCAACATCG
<i>C. auris- YCF1</i>	Forward (5'-3'): AGTCCGAGAACAAGGAGACGA AGG Reverse (5'-3'): TGGCAACTGACAAGCACTGAC
<i>C. auris- ALS7</i>	Forward (5'-3'): AGTGATTCTATCTTCGCCGCTTGG Reverse (5'-3'): TGGCAATGGAAGTGGCAGTGATAC
<i>C. auris- SCF1</i>	Forward (5'-3'): CCAAAGGGTGAACAGCCAGAAGG Reverse (5'-3'): ACAGAAGGAGCAGGAGCAGGTC

ml) with equal drug quantities (7.4, 14.8, 29.6, 59.2  $\mu\text{M}$  BE, and 209  $\mu\text{M}$  FLZ) using a micropipette. The mixture was then added dropwise to the surface of the Plate and incubated at 37 °C for 3–4 days (Kumar et al. 2015). A control group without drugs was included. We analyzed the effect of the drugs on hemolytic secretion using the HZ value, which was calculated as the colony diameter divided by the sum of the precipitation circle and the colony diameters. An HZ value of 1.0 indicated no hemolytic activity, and no precipitation circle was observed around the colony. An HZ value < 1.0 indicates the presence of a precipitation circle around the colony. A smaller HZ value correlates with a larger precipitation circle, indicating a more active secretion of hemolysin by *C. auris*.

### XTT assay

The XTT assay was employed to assess the ability of the drug to inhibit *C. auris* biofilms. The fungal suspension was adjusted to  $2 \times 10^6$  cells/ml, and the drug solution was prepared using a serial two-fold dilution method. The final concentrations ranged from 7.4–947.3  $\mu\text{M}$  for BE and 209–3343.5  $\mu\text{M}$  for FLZ. We combined 100  $\mu\text{l}$  of fungal suspension with 100  $\mu\text{l}$  of drug solution in each well, then incubated the plates at 37 °C for 24 h. Absorbance at 492 nm was measured for each well using an enzyme labeler. After incubation, we added 50  $\mu\text{l}$  of XTT (740.2  $\mu\text{M}$ ) and menadione (10  $\mu\text{M}$ ) (MackLin Bio-Chem Technology Co., Ltd, Shanghai, China) to each well and incubated for 2 h in the absence of light. The OD measurements for each well were taken at 492 nm using a spectrophotometer (Larkin et al. 2017).

### Violet crystal assay

The concentration of *C. auris* during the logarithmic growth phase was adjusted to  $2 \times 10^6$  cells/ml. Subsequently, 7.4, 14.8, 29.6, and 59.2  $\mu\text{M}$  of BE and 209  $\mu\text{M}$  of FLZ were added to the *C. auris* suspension. A control group was also established without medication. After co-incubating the drug solution and fungal suspension for 24 h, we removed any non-adherent planktonic cells by rinsing the wells twice with

sterile PBS. The wells were incubated with crystal violet staining solution (Yeasen Biotechnology Co., Ltd., Shanghai, China) for 45 min, washed twice with sterile PBS, and then incubated with 95% (v/v) ethanol for 45 min. Finally, the absorbance of each well was measured at 560 nm using a microplate reader (Zhang et al. 2024).

### SEM

The coverslips were treated with 75% ethanol and placed in six-well plates. Cells of *C. auris* in the logarithmic growth phase were added at a concentration of  $2 \times 10^6$  cells/ml. The *C. auris* suspensions were treated with 7.4, 14.8, 29.6, and 59.2  $\mu\text{M}$  of BE and 209  $\mu\text{M}$  of FLZ, while a control group without medication was established. After being cultured for 24 h at 37 °C, non-adherent cells were rinsed with sterile PBS buffer and then immersed in pre-chilled 2.5% glutaraldehyde for a minimum of 2 h. The samples underwent dehydration in 30%, 70%, 95%, and 100% ethanol for 10 min. Following adequate drying at room temperature, the samples were gold-coated, observed, and photographed using SEM (Larkin et al. 2017). Similar processing was applied to pig skin samples.

### CLSM

The concentration of *C. auris* in the logarithmic growth phase was adjusted to  $2 \times 10^6$  cells/ml. Subsequently, *C. auris* suspension was treated with 7.4, 14.8, 29.6, 59.2  $\mu\text{M}$  of BE and 209  $\mu\text{M}$  of FLZ. A control group without medication was also included. After incubating at 37 °C for 24 h, non-adherent fungal cells were removed by rinsing with sterile PBS. Subsequently, a FunXite-1 dual-color fluorescent active probe (Lumiprobe Corporation, USA) was added, and the cells were stained for 1 h under light protection (Larkin et al. 2017). Fluorescent expression was observed using an FV3000 CLSM (Olympus, Shinjuku, Tokyo, Japan).

### Flow cytometry

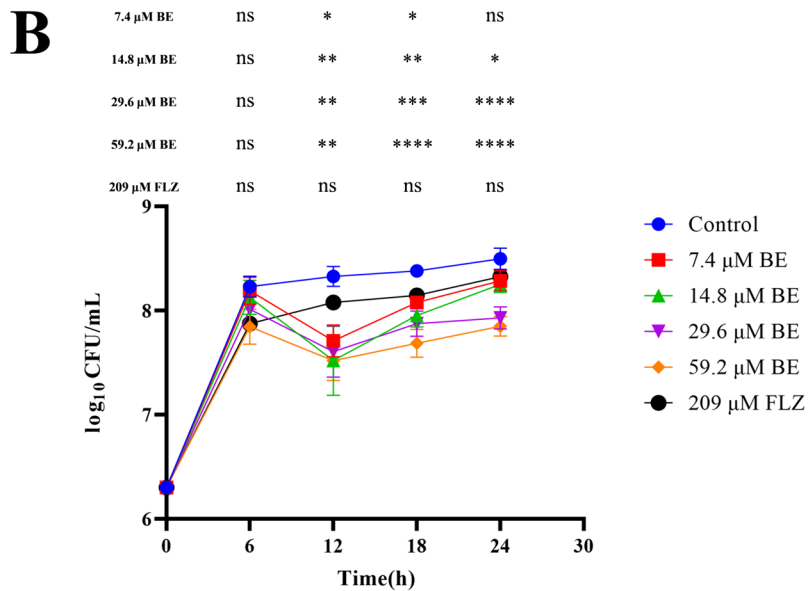
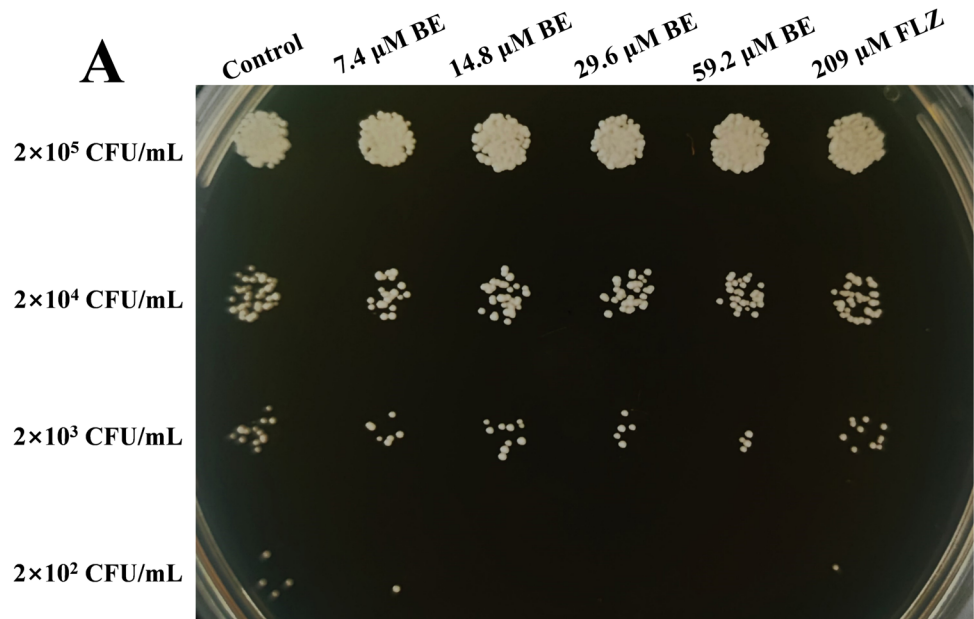
The concentration of *C. auris* cells was adjusted to  $2 \times 10^6$  CFU/ml using PBS, followed by centrifugation at  $825 \times g$  for 5 min and resuspension in fresh PBS. Rhodamine 6G was added at a final concentration of 10  $\mu\text{M}$  (Macklin Bio-Chem Technology Co., Ltd, Shanghai, China) to the *C. auris* cultures, which were then incubated at 35 °C for 50 min. Rhodamine 6G uptake was stopped by placing the *C. auris* on ice, followed by centrifugation at  $825 \times g$  for 5 min. The collected cells underwent three washes with PBS and then treated with different concentrations of BE (7.4, 14.8, 29.6, 59.2  $\mu\text{M}$ ) or FLZ (209  $\mu\text{M}$ ). The fluorescence

**Table 2** MIC of BE against *C. auris*

Strain	MIC( $\mu\text{M}$ )	MIC <sub>80</sub> ( $\mu\text{M}$ )	MFC ( $\mu\text{M}$ )	SMIC ( $\mu\text{M}$ )
C1	0.93–1.85	0.46	7.4	29.6–59.2
C2	0.93–1.85	0.46	7.4	59.2
C3	1.85	0.93	7.4	118.4
C4	1.85	0.93	7.4	29.6–59.2

MIC Minimum inhibitory concentration, MFC Minimum fungicidal concentration, SMIC Sessile minimum inhibitory concentration

**Fig. 1** Inhibitory effect of baicalein (BE) on *C. auris* growth. **A** After co-culturing for 24 h, the growth-inhibiting impact of BE on different concentrations of *C. auris* was detected using spot assay. **B** BE and *C. auris* were cultured together for different time periods (0, 6, 12, 18, and 24 h), and the impact of BE on inhibiting the growth of *C. auris* was assessed by counting the number of colonies. All data are presented as mean  $\pm$  SD: ns = not significant, \* $P$  < 0.05, \*\* $P$  < 0.01, \*\*\* $P$  < 0.001, \*\*\*\* $P$  < 0.0001 vs. Control group



intensity of R6G in cells (10,000 cells) was measured using flow cytometry (BD FACSCelesta, USA) with excitation at 488 nm and emission at 525 nm at time points: 10, 30, 60, 90, and 120 min (Zhang et al. 2024).

### Live/dead fluorescent staining

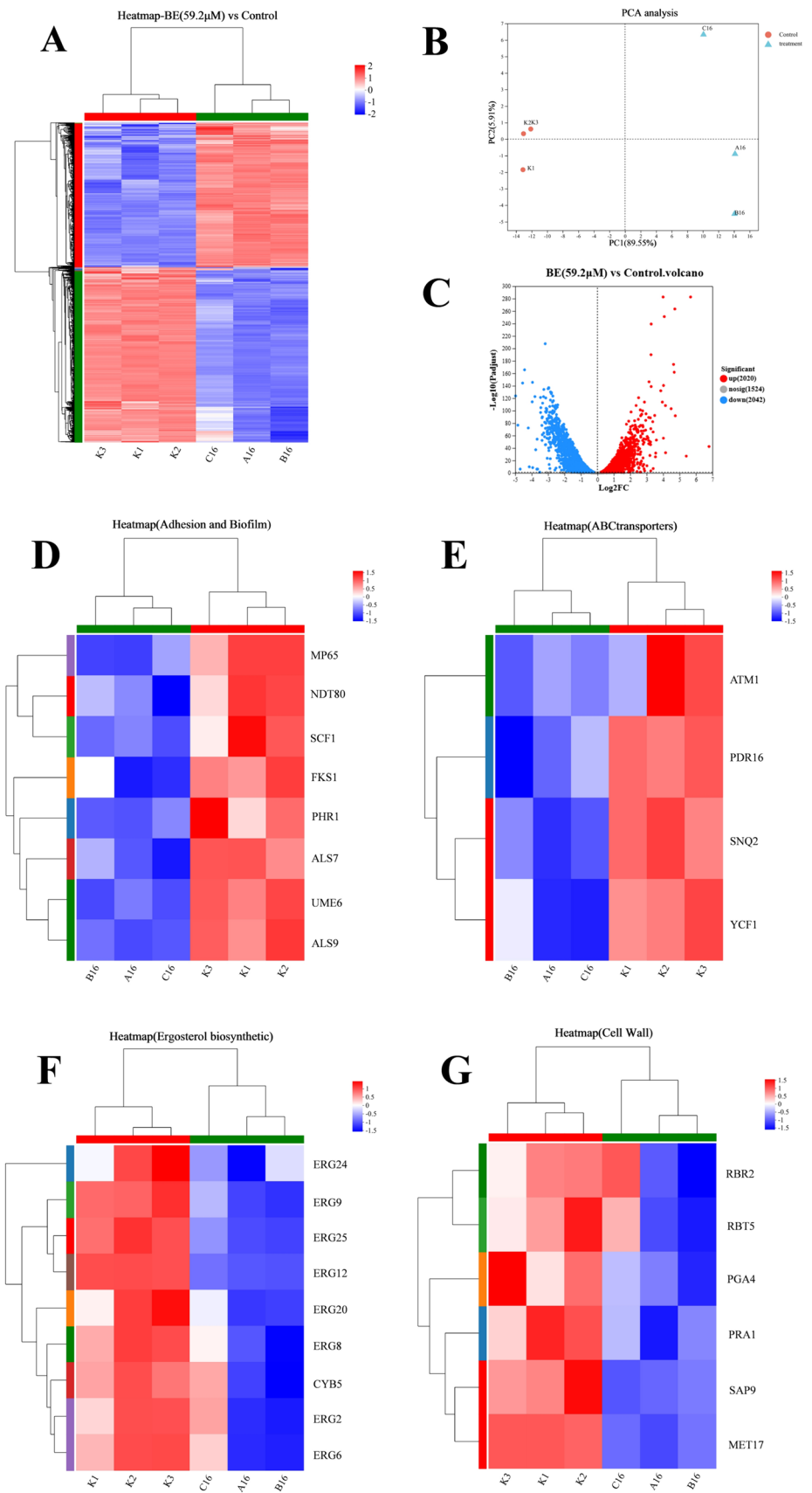
During the logarithmic growth phase, the concentration of *C. auris* was adjusted to  $2 \times 10^6$  cells/ml. Subsequently, BE at concentrations of 7.4, 14.8, 29.6, and 59.2  $\mu$ M, along with FLZ at 209  $\mu$ M, were added to the *C. auris* suspensions. Additionally, a control group without any drug was established. Following a 24-h incubation period, the biofilms

underwent staining with FDA (10  $\mu$ M) and PI (10  $\mu$ M, Beyotime Biotechnology Co., Ltd., Shanghai, China) for approximately 5 min. The cells were subsequently rinsed with sterile PBS to remove excess staining (Sun et al. 2022). Fluorescent expression was examined using a DMi8 microscope (Leica, Wetzlar, Hesse, Germany) at a magnification of 200 $\times$ .

### Reactive oxygen species

The fungal cells ( $2 \times 10^6$  cells/ml) were treated with 7.4, 14.8, 29.6, 59.2  $\mu$ M of BE and 209  $\mu$ M of FLZ for 24 h at 37  $^{\circ}$ C. No rats were allocated to the control group. Samples were stained using the ROS Assay Kit (Beyotime

**Fig. 2** Baicalein (BE) regulates the expression of genes associated with *C. auris*. **A** Heatmap of clustering analysis of all genes. **B** Principal components analysis (PCA) mapping of control and BE samples. **C** Volcano plots between BE and control groups. **D–G** Heatmap of clustering analysis of virulence-related genes





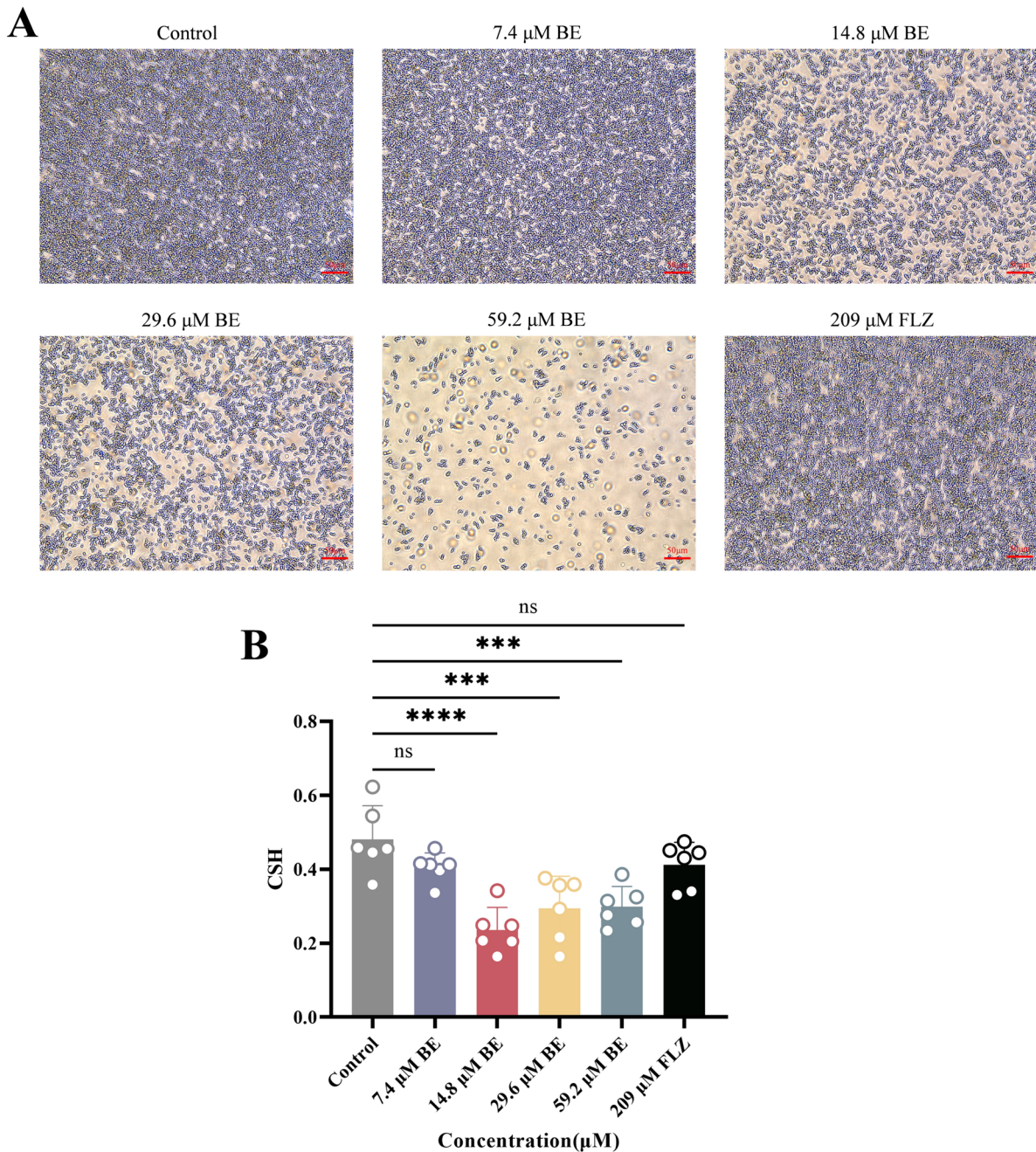


**Fig. 3** Baicalein (BE) inhibits flocculation and cell surface hydrophobicity (CSH) of *C. auris*. **A** Images represent flocculation of *C. auris*. Scale bars 50  $\mu\text{m}$ . **B** CSH of *C. auris* was measured by the water-

hydrocarbon two-phase method. All data are presented as mean  $\pm$  SD: ns = not significant, \*\*\* $P$  < 0.001, \*\*\*\* $P$  < 0.0001 vs. Control group

Biotechnology Co., Ltd, Shanghai, China) for 20 min at 37  $^{\circ}\text{C}$ . Excess 2',7'-Dichlorodihydrofluorescein diacetate (DCFH-DA) was removed with sterile PBS (Lei et al. 2023). Fluorescence was observed using a DMi8 microscope (Leica, Wetzlar, Germany) at  $\times 630$  magnification.

**Cell wall assay**

The fungal cells ( $2 \times 10^6$  cells/ml) were treated with 7.4, 14.8, 29.6, 59.2  $\mu\text{M}$  of BE and 209  $\mu\text{M}$  of FLZ for 24 h at 37  $^{\circ}\text{C}$ . Subsequently, the fungal cells were collected, washed with sterile PBS, and treated with a fungal suspension in calcofluor white (CFW, 10  $\mu\text{M}$ , Sigma-Aldrich, Shanghai, China). Staining for chitin content was conducted in the dark



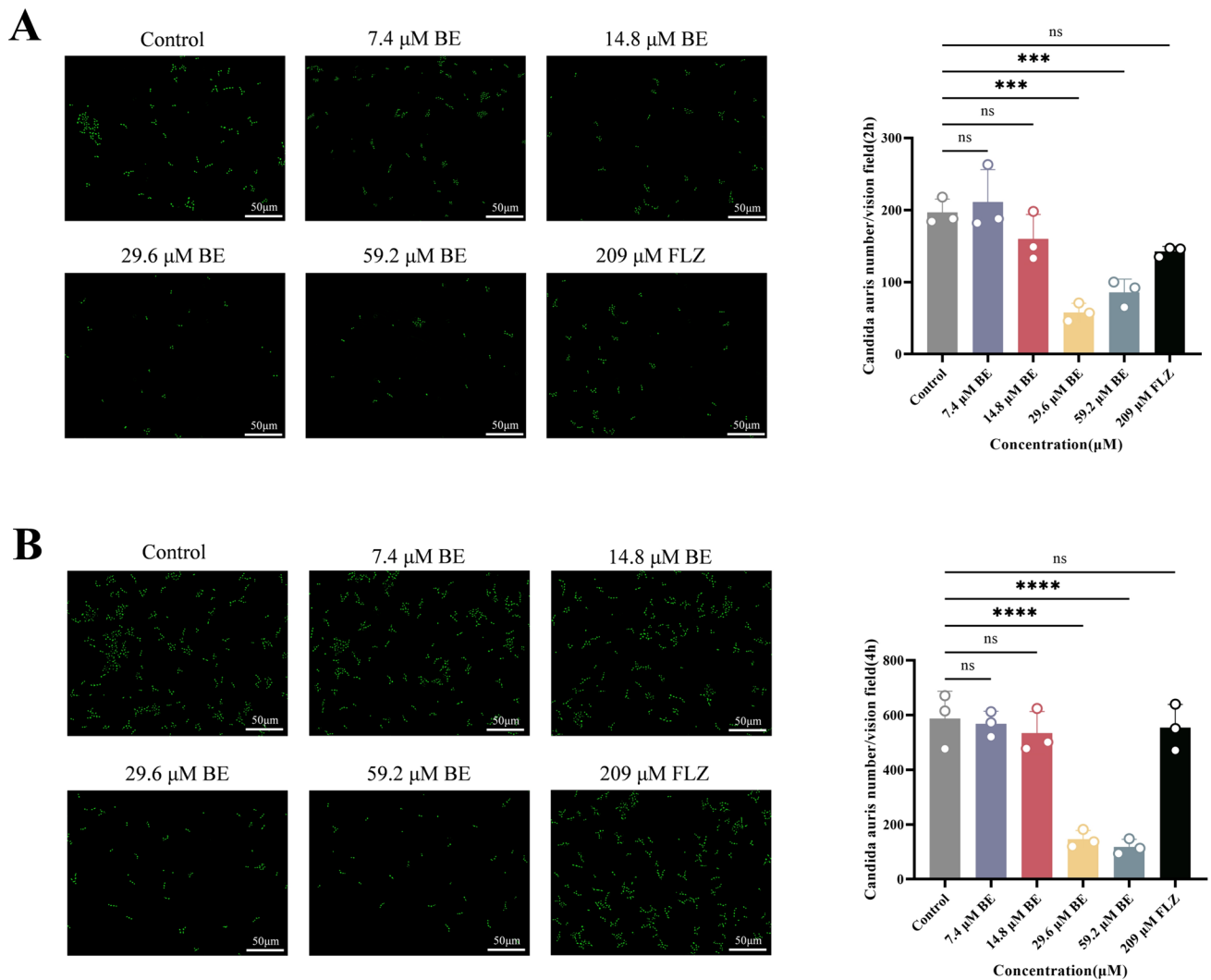


**Fig. 4** Baicalein (BE) inhibits the adhesive ability of *C. auris*. **A** Images represent the state of *C. auris* adhesion at 2 h. Scale bars 50 μm. Quantification of *C. auris* number by Image J. **B** Images represent the state of *C. auris* adhesion at 4 h. Scale bars 50 μm.

Quantification of *C. auris* number by Image J. All data are presented as mean ± SD: ns = not significant, \* $P < 0.05$ , \*\*\* $P < 0.001$ , \*\*\*\* $P < 0.0001$  vs. Control group

at 37 °C for 30 min. As previously stated, samples were treated with aniline blue (Solarbio Science & Technology Co., Ltd, Beijing, China) and incubated in the dark at room temperature for 60 min. (Lei et al. 2023). Fluorescence was examined using a DMi8 microscope (Leica, Wetzlar, Germany) at ×630 magnification.

### Aggregation assay

The concentration of *C. auris* during its logarithmic growth phase was adjusted to  $2 \times 10^8$  cells/ml (Ramos et al. 2023). Subsequently, 7.4, 14.8, 29.6, and 59.2 μM, along with FLZ at 209 μM, were added to the *C. auris* suspension. A control group that received no treatment was also included. The fungal suspensions underwent incubation at 37 °C for 120 min.

Subsequently, the liquid was examined with a DMi8 microscope (Leica, Wetzlar, Hesse, Germany) at a magnification of ×200.

### Porcine skin model

The skin (the skin was obtained from a local abattoir) was cleaned with PBS and 75% ethanol and then shaved. Using a biopsy punch, 12 mm full-thickness skin samples were collected and placed in 12-well plates containing 3 mL of Dulbecco's modified Eagle's medium (DMEM) supplemented with 10% Fetal Bovine Serum (FBS, Hyclone, Logan, UT, USA). The samples were incubated for 6 h at 37 °C with 5% CO<sub>2</sub>. After rinsing in PBS and thorough drying, a 1 ml paraffin barrier was applied to the inner surface of the DMEM at

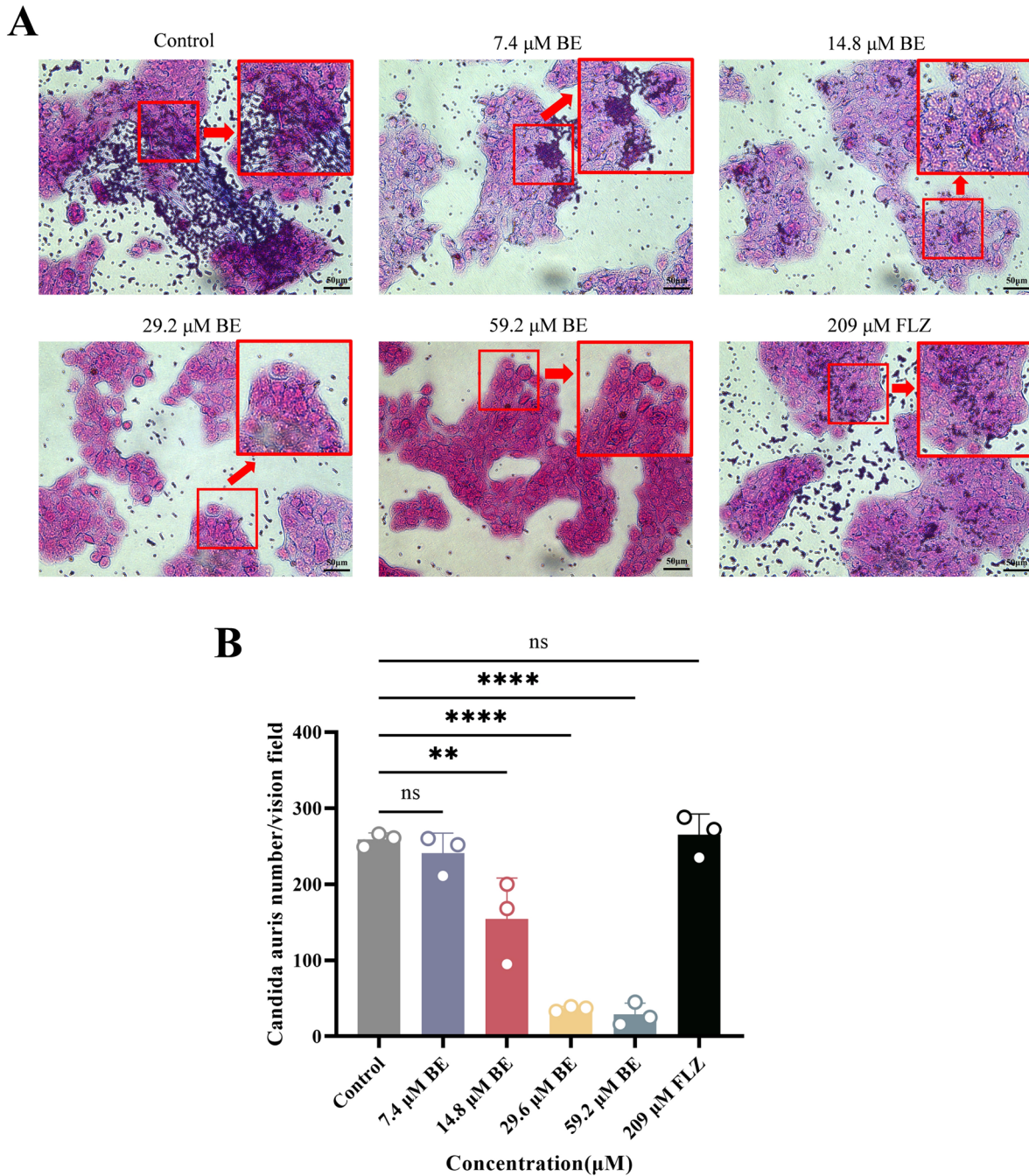


**Fig. 5** Baicalein (BE) inhibits adhesion of *C. auris* to Human Keratinocytes Cells (HaCaT) cells. **A** Images represent *C. auris* adhering to the surface of HaCaT cells. **B** Quantification of *C. auris*

number by Image J. All data are presented as mean ± SD: ns = not significant, \**P* < 0.05, \*\**P* < 0.01, \*\*\**P* < 0.001, \*\*\*\**P* < 0.0001 vs. Control group

the epidermal interface. *C. auris*, suspended in medium (10<sup>7</sup> cells/ml), was applied to the skin surface (10 μl). Following a 24-h incubation at 37 °C with 5% CO<sub>2</sub> but without humidity, the skin samples were prepared for SEM and plated for viability assessment (Horton et al. 2020).

### G. mellonella larvae infection model

The *G. mellonella* larvae (Jiacheng Insect Breeding, Guilin, China) were stored at 4 °C and revived at room temperature for 30 min before the experiments. Based on the survival study, a median lethal dose (LD50) of 7 × 10<sup>6</sup> cells/ml was determined for *G. mellonella* larvae. Larval-killing assays

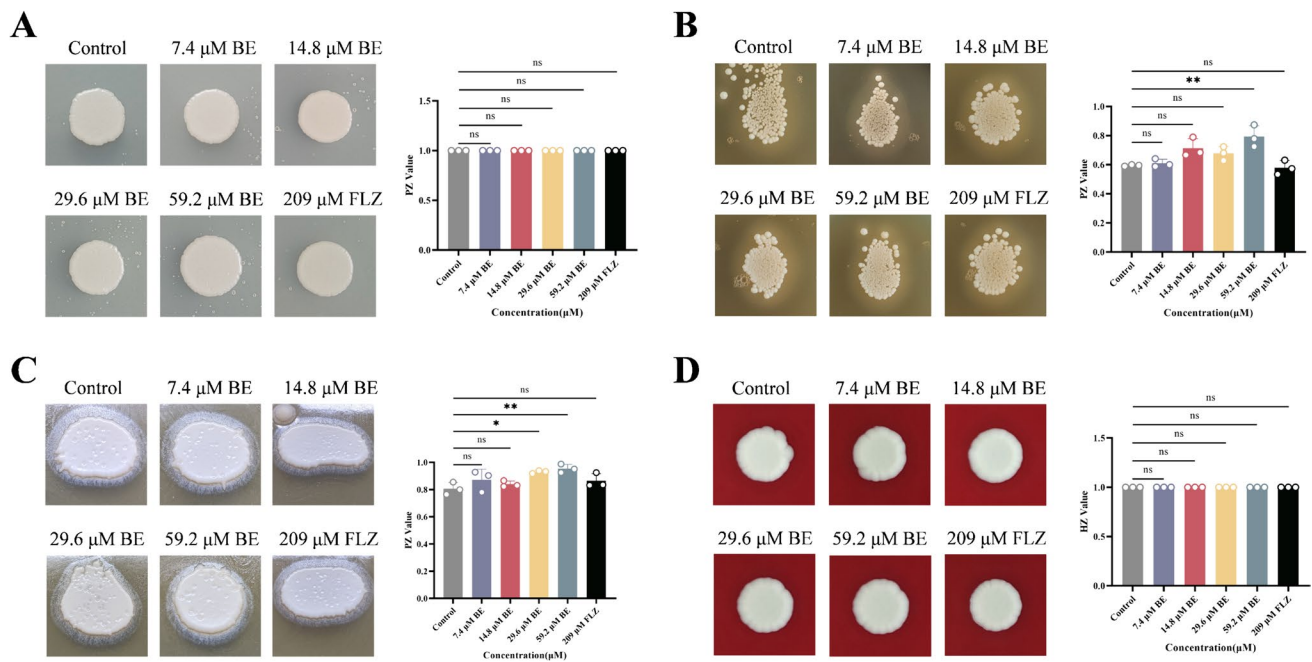


**Fig. 6** Baicalein (BE) inhibits partial hydrolase secretion in *C. auris*. **A** Images represent the growth of *C. auris* on a medium containing bovine serum albumin. Analyses the effect of BE on proteinase activity based on zone of precipitation (PZ) values. **B** Images represent the growth of *C. auris* on a lipase medium. Analyses the effect of BE on esterase activity based on PZ values. **C** Images represent the growth

of *C. auris* on an egg yolk agar base. Analyses the effect of BE on phospholipase activity based on PZ values. **D** Images represent the growth of *C. auris* on a Columbia CNA Blood Agar Plate. Analyses the effect of BE on hemolytic activity based on zone of hemolytic activity (HZ) values. All data are presented as mean  $\pm$  SD: ns = not significant, \* $P < 0.05$ , \*\* $P < 0.01$  vs. Control group

were conducted at 37 °C, with 10 randomly assigned larvae to each group inoculated with 10  $\mu$ l of *C. auris* ( $7 \times 10^6$  cells/ml) through the last right proleg. Two hours later, the larvae were injected with sterile PBS, BE (7.4, 14.8, 29.6, 59.2  $\mu$ M) and FLZ (209  $\mu$ M) through the last left proleg. The treated larvae were then kept in darkness at 37 °C for 5 days, with daily recording of deceased larvae numbers (Pan et al. 2021).

## RT-qPCR

Total cDNA extracted from *C. auris* was used to synthesize cDNA following the instructions of the manufacturer for the reverse transcription kit (Yeasen Biotechnology Co., Ltd., Shanghai, China). Table 1 depicts the primer sequences. The RT-qPCR amplification was conducted using a Light Cycler  $\text{\textcircled{R}}$  96 for fluorescence quantification, with the following program: initial denaturation at 95 °C for 5 min, followed by 40 cycles of denaturation at 95 °C for 10 s, annealing at 50–60 °C for 20 s, and extension at 72 °C for 20 s. Gene expression levels were analyzed using the relative quantification method based on the cycle threshold values ( $2^{-\Delta\Delta C_t}$ ) (Wu et al. 2023).

## Statistical analysis

The presented data are expressed as the mean  $\pm$  standard deviation of at least three biological replicates. Statistical analysis utilized Graphpad Prism 9.5 and SPSS 23.0, employing one-way ANOVA followed by LSD or Welch's method. Statistical significance was determined at  $P < 0.05$ .

## Results

### BE demonstrates clear inhibitory effects against *C. auris*

We evaluated the inhibitory and fungicidal effect of BE on *C. auris* by determining the MIC and MFC values against four strains. The results showed MIC values ranging from 0.93–1.85  $\mu$ M (Table 2) for all strains and MFC values were 7.4  $\mu$ M (Table 2), indicating strong growth inhibition and fungicidal activity by BE across the tested strains. *C. auris* strains with the lowest MIC values (*C. auris* strains C1) were selected for further virulence experiments.

To investigate the effect of BE on the growth of *C. auris*, we used the spot assay to examine the effect of different concentrations of BE on the growth of *C. auris*. This method

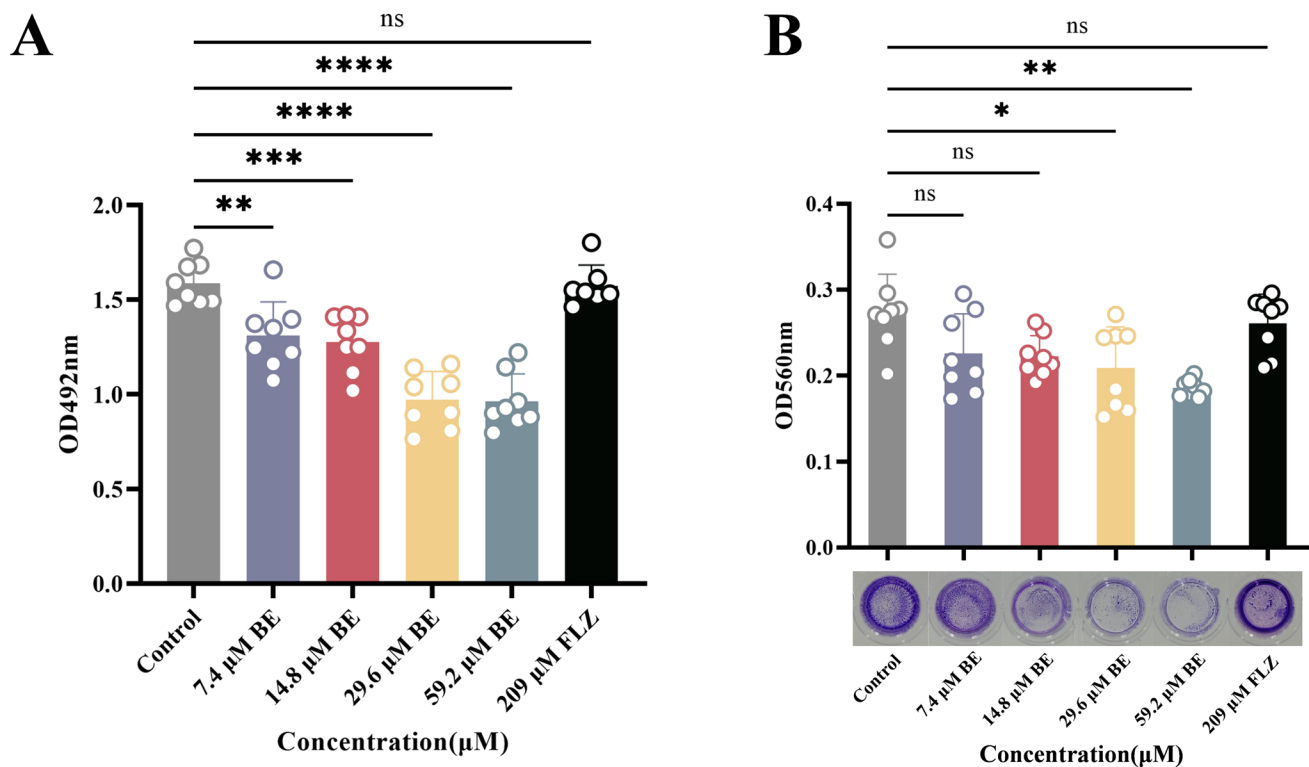


**Fig. 7** Baicalein (BE) inhibits *C. auris* biofilm formation. **A** Images represent the effect of BE on the metabolic viability of *C. auris*, measured at 492 nm. **B** Images represent the effect of BE on the biomass of *C. auris* biofilms, measured at 560 nm; The biomass of bio-

films formed by *C. auris* was measured in 96-well plates using crystal violet staining. All data are presented as mean  $\pm$  SD; ns = not significant, \* $P < 0.05$ , \*\* $P < 0.01$ , \*\*\* $P < 0.001$ , \*\*\*\* $P < 0.0001$  vs. Control group

is crucial for detecting fungal activity by observing colony growth on a solid agar medium. Our study revealed that varying concentrations of *C. auris* treated with 7.4 and 14.8  $\mu$ M of BE along with 209  $\mu$ M of FLZ showed no significant change in colony growth compared to those in the control group. However, at 29.6  $\mu$ M or 59.2  $\mu$ M BE concentrations, *C. auris* growth was significantly inhibited, indicating the inhibitory effect of BE on *C. auris* growth (Fig. 1A).

Time-growth studies showed the time and concentration-dependent antimicrobial activity of a drug, making it applicable as a microbiostatic drug. Here, we investigated the antifungal effects of BE on *C. auris* at different time intervals. These results showed that the antifungal effect of BE peaked at the 12th hour. However, over time, this effect diminished while still exhibiting a dependence on drug concentration (Fig. 1B). These findings suggest that BE may have a moderate antifungal effect on *C. auris*.

### Effect of BE on the transcriptomics profile of *C. auris*

To gain further insight into the potential molecular mechanisms of BE against *C. auris*, we conducted transcriptome sequencing analysis on *C. auris* samples from the control and BE treatment groups using the Illumina high-throughput

sequencing platform. Principal component analysis (Fig. 2B) revealed significant differences between these groups, indicating that pharmacological interventions can affect transcriptional patterns. Significantly, compared to the control group, genes in the treatment group exhibited a significant rightward shift.

This study focused on genes that exhibited differential expression in the BE treatment group (59.2  $\mu$ M) compared to the control group. Overall, 4,062 differentially expressed genes, comprising 2,020 upregulated and 2,042 down-regulated genes, were identified in the BE treatment group (Fig. 2A and C). This suggests that BE intervention significantly changed the gene expression of *C. auris*, highlighting the comprehensive effect of BE on *C. auris* and indicating its considerable potential against *C. auris* infections in the future. Additional clustering analysis of these genes, depicted in the heatmap, indicated that BE-regulated genes associated with adhesion, biofilm formation, efflux pumps, cell membranes, and cell walls in *C. auris* (Fig. 2D-G) (Jakab et al. 2024).



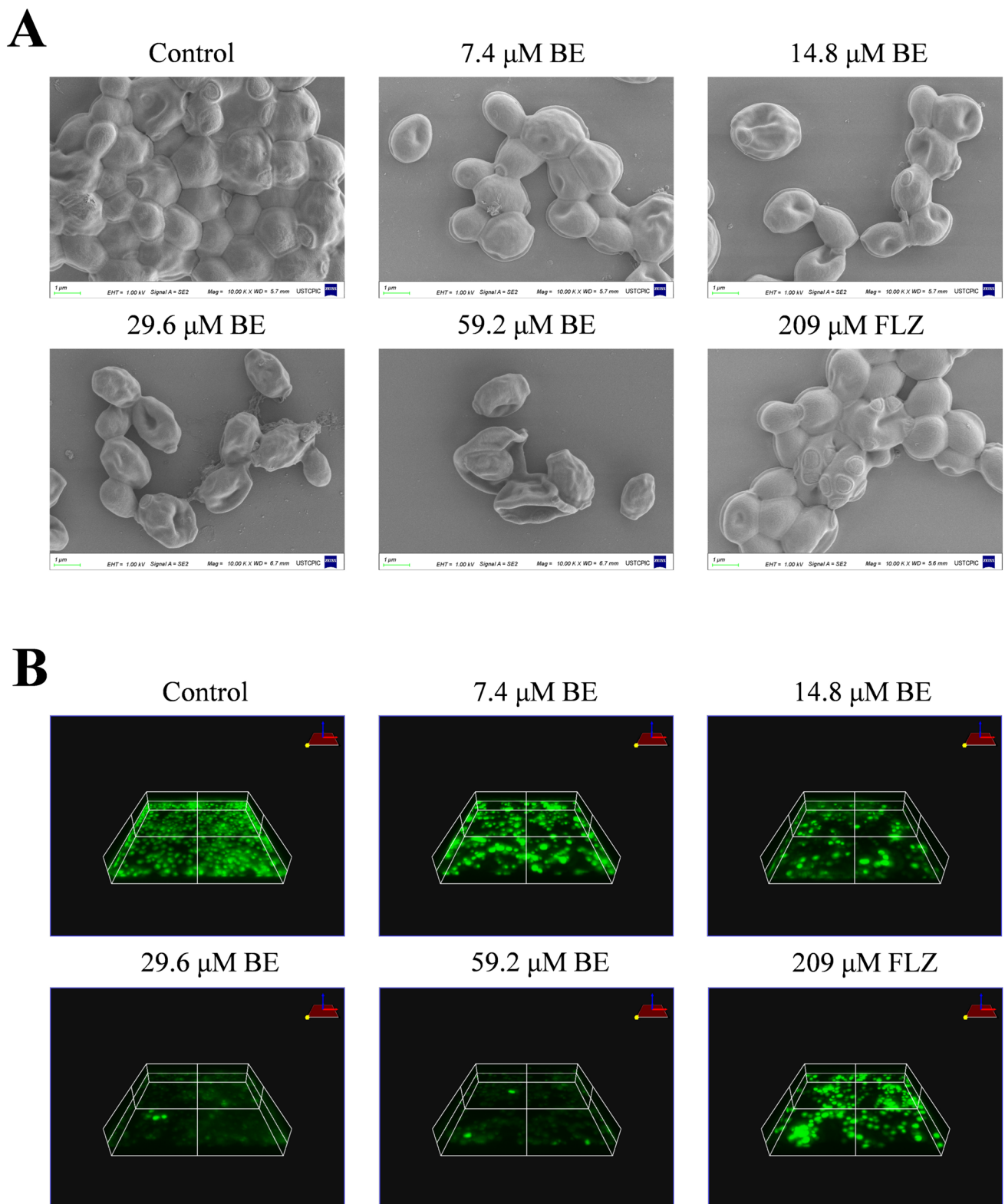


**Fig. 8** Baicalein (BE) disrupts the morphological structure of *C. auris* biofilm. **A** Images represent the biofilms of *C. auris* under scanning electron microscope (SEM) observation. **B** Images represent

the morphological structure of *C. auris* biofilms under confocal laser scanning microscope (CLSM) observation



## BE inhibits flocculating ability, cell surface hydrophobicity, and adherence of *C. auris*

Upon examining the flocculent under an inverted microscope, it was discovered that a significant number of *C. auris* adhered and accumulated into clusters in the control and 209  $\mu\text{M}$  FLZ groups. Similarly, many *C. auris* adhered and formed clusters in the 7.4 and 14.8  $\mu\text{M}$  BE concentration groups, while only a few clusters were observed in the 29.6 and 59.2  $\mu\text{M}$  BE concentration groups (Fig. 3A).

The positive correlation between CSH and adhesion has established CSH as a reliable indicator of adhesion capability. Our results showed significantly lower relative hydrophobicity of the cell surface in the BE group (14.8, 29.6, and 59.2  $\mu\text{M}$  BE) but not in the FLZ group (Fig. 3B).

Early adhesion plays a pivotal role as a virulence factor in *Candida* spp. Fluorescence microscopy examination revealed that a small quantity of *C. auris* adhered to the coverslips after a two-h incubation. Comparatively, the treatment group exhibited significantly fewer *C. auris* adhering to the coverslips than that of the treatment group (Fig. 4A). After 4 h of incubation, a significant increase was observed in the number of *C. auris* adhered to the coverslips under fluorescence microscopy. In the control and 209  $\mu\text{M}$  FLZ groups, a significant number of adherent *C. auris* were observed, forming clusters. Increasing the BE concentration led to a decrease in the number of adherent *C. auris* cells, accompanied by a corresponding reduction in adherent clusters (Fig. 4B). Furthermore, BE reduced the adhesion of *C. auris* to HaCaT cells. In bright field observation, a significant number of *C. auris* adhered to the HaCaT cell surface in the control group and 209  $\mu\text{M}$  FLZ group. However, as BE concentration increased, the number of *C. auris* cells and their adhesion to HaCaT cells decreased. At BE concentrations of 29.6  $\mu\text{M}$  and 59.2  $\mu\text{M}$ , respectively, a significant decrease was observed between the number of *C. auris* and their adhesion ability (Fig. 5A and B).

## BE inhibits partial hydrolase secretion

This study examined the virulence characteristics of *C. auris*. The results revealed that the strain did not show proteinase or hemolytic activities, with only weak levels of phospholipase activities observed and strong levels of esterase activity detected. A significant inhibitory effect on phospholipase secretion in *C. auris* was only observed at BE concentrations of 29.6  $\mu\text{M}$  and 59.2  $\mu\text{M}$ . Similarly, esterase secretion in *C. auris* was inhibited only at a BE concentration of 59.2  $\mu\text{M}$  (Fig 6A–D).

## BE inhibits *C. auris* biofilm formation

Biofilms are created when a group of cells adhere together to produce a matrix of extracellular polymeric substances (EPS). We assessed the inhibitory effect of BE on *C. auris* biofilms by determining SMIC through the XTT method. Figure 7A depicts the inhibitory effect of BE on *C. auris*. The OD value at 492 nm for *C. auris* indicated that the SMIC ranged from 29.6–118.4  $\mu\text{M}$ , indicating that BE can impede the formation of *C. auris* biofilm to some extent.

Biofilms were detected using crystal violet staining, with *C. auris* staining levels assessed at the base of a 96-well plate. OD was measured at 560 nm using a microplate reader. The presence of crystal violet-stained *C. auris* biofilms was indicated by a purple residue at the bottom of the 96-well plate. The control and 209  $\mu\text{M}$  FLZ-treated groups displayed strong crystal violet staining at the bottom of the plate, indicating robust *C. auris* biofilm growth. Conversely, BE-treated wells exhibited reduced crystal violet staining in a concentration-dependent manner (Fig. 7B). The OD value at 560 nm confirmed that BE inhibited *C. auris* biofilm growth and biomass reduction.

The inhibitory effect of BE on *C. auris* biofilms was validated using SEM. The control and 209  $\mu\text{M}$  FLZ groups showed distinct oval-shaped yeast morphology in *C. auris*. However, cells exposed to BE at a concentration of 29.6  $\mu\text{M}$  and 59.2  $\mu\text{M}$  exhibited significantly altered yeast cell topography, indicating an impaired ability to divide (Fig. 8A).

The inhibitory effect of BE on *C. auris* biofilm formation was examined with CLSM. FUNXite-1, known for binding to the cell membrane and undergoing transformation within the cell, emitted green fluorescence. OLYMPUS FV3000 software and 3D reconstruction technology were utilized to generate a 3D view of the CLSM image. The Figure illustrates that the biofilm structure in control and 209  $\mu\text{M}$  FLZ groups remained intact, with cells in good condition and exhibiting vigorous growth, resulting in thicker biofilm formation. However, the biofilm thickness of the 7.4  $\mu\text{M}$  and 14.8  $\mu\text{M}$  BE groups were relatively reduced. Additionally, a significant decrease was observed in the thickness of the *C. auris* biofilm, as well as a reduction in the quantities of cells in the 29.6  $\mu\text{M}$  BE and 59.2  $\mu\text{M}$  BE groups (Fig. 8B). These findings suggest that the absence of complete biofilm formation.

## BE suppresses resistance in *C. auris* biofilm

Flow cytometry results showed that initial intracellular fluorescence levels were similar across all groups, gradually decreasing over time. However, the rate of fluorescence decline in the 29.6  $\mu\text{M}$  BE and 59.2  $\mu\text{M}$  BE groups was significantly slower than that of the control and 209  $\mu\text{M}$

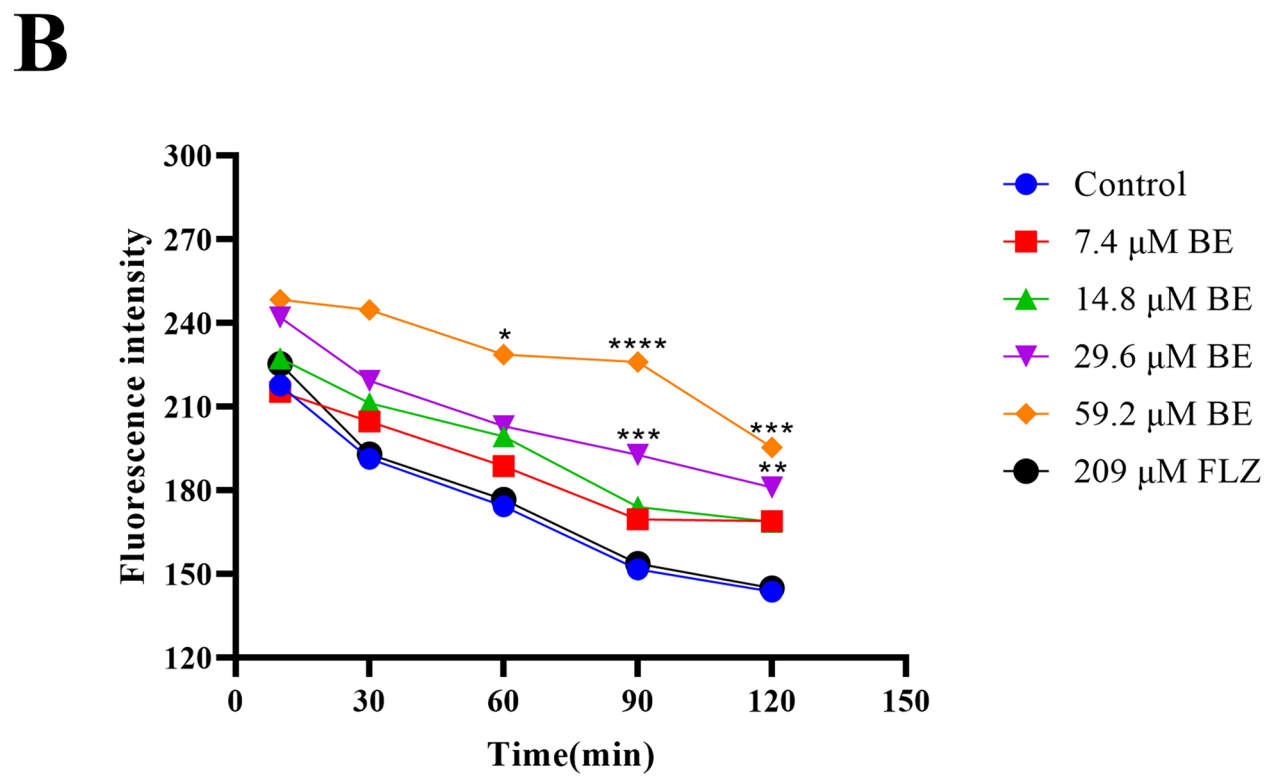
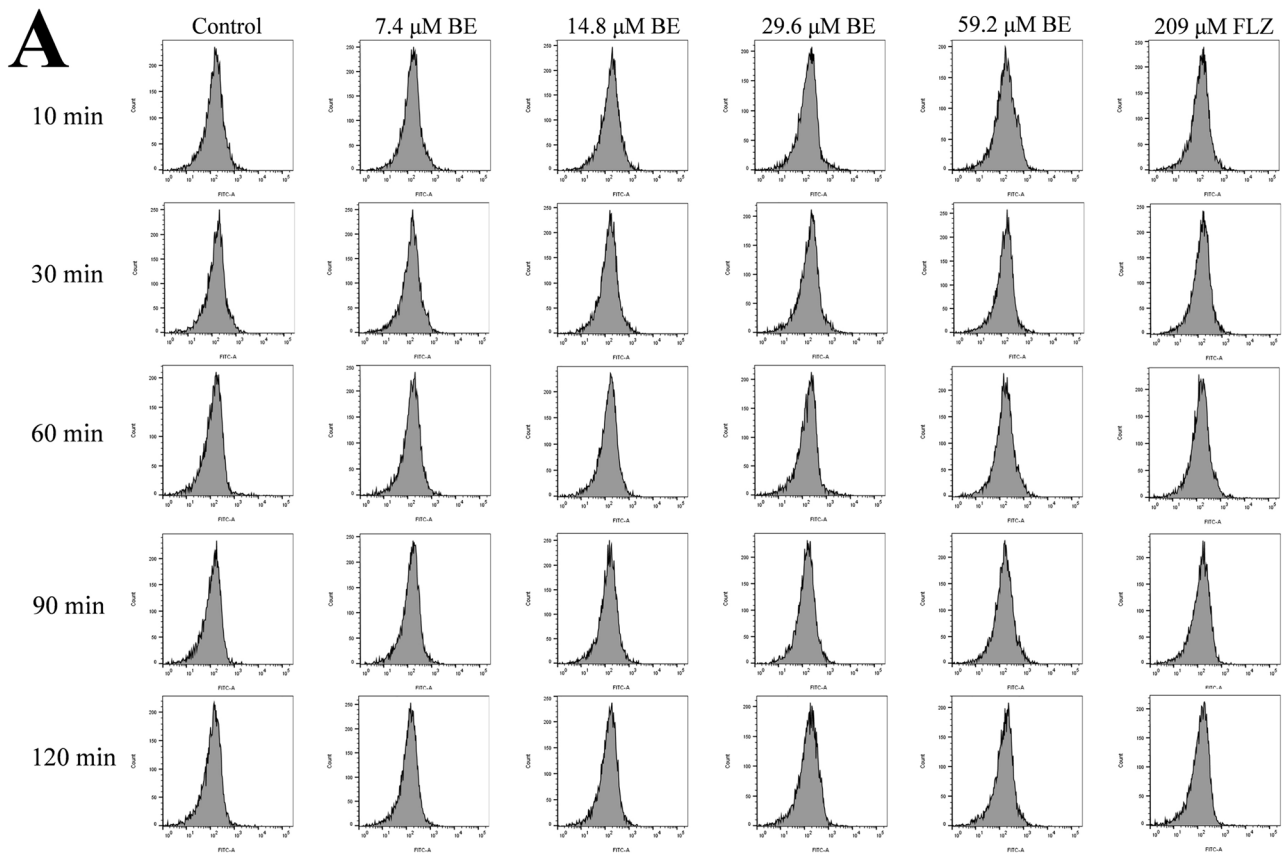


**Fig. 9** Effect of baicalein (BE) on efflux transporters in *C. auris*. **A** Flow cytometry images represent *C. auris* efflux pump protein expression after BE treatment at different times. **B** The mean fluorescence strength of the excretory transport protein in *C. auris*. All data are presented as mean  $\pm$  SD: \* $P < 0.05$ , \*\* $P < 0.01$ , \*\*\* $P < 0.001$ , \*\*\*\* $P < 0.0001$  vs. Control group

FLZ groups (Fig. 9), indicating that BE may inhibit the efflux pump activity of *C. auris*.

### BE induces the apoptosis of *C. auris*

To determine the effect of BE on *C. auris* cell viability, we analyzed changes in differential expression between live and dead cells. The control group and 209  $\mu$ M FLZ group exhibited intense green fluorescence, indicating mature biofilm formation. After incubation with 7.4  $\mu$ M BE and 14.8  $\mu$ M BE, *C. auris* showed a reduction in cell numbers, with most cells expressing green fluorescence, indicating an active state. However, incubation with 29.6  $\mu$ M BE and 59.2  $\mu$ M BE resulted in a significant increase in red fluorescence, indicative of an increase in dead cells (Fig. 10). Mitochondria generate ROS, which can affect cell membranes and walls integrity. Therefore, we quantified ROS production, as depicted in the Figure. Figure 11A and B depict a significant increase in fluorescence following BE treatment. Particularly, 74.32% and 78.44% of cells tested positive for ROS after treatment with 29.6  $\mu$ M BE and 59.2  $\mu$ M of BE, respectively. However, other groups exhibited considerably lower ROS levels. These findings indicate that BE significantly enhances ROS production.

### BE damages the cell wall integrity and inhibits *C. auris* aggregation

The fungal cell wall plays a crucial role in maintaining cell shape and controlling polarized growth. *Candida* yeasts can modify their cell wall composition and structure in response to environmental changes. Figure 12A illustrates that before BE treatment, CFW was uniformly distributed in yeast cells. However, after treatment with 29.6  $\mu$ M BE, and 59.2  $\mu$ M BE, a higher concentration of CFW was observed in the outer layer of *C. auris* cells (Malavia-Jones et al. 2023), particularly at the budding end (indicated by red arrows). CFW fluorescence analysis showed an increase in chitin content following BE treatment. Additionally, aniline blue staining assay results indicated a reduction in total glucan levels after BE treatment (Fig. 12B). These results indicated that BE altered the structure of the *C. auris* cell wall.

Aggregation has recently been identified as an important virulence factor in *C. auris* and is closely associated with the cell wall. (Bing et al. 2024). The results showed that higher BE concentration led to significant inhibition of *C. auris* aggregation. Certain inhibition was also observed in the FLZ group (Fig. 13).

### BE inhibits *C. auris* colonization on porcine skin and decreases its infection to *G. mellonella* larvae

A porcine skin model was created to simulate *C. auris* growth in the skin niche (Fig. 14A). The selection of pig skin was based on its similarity to human skin regarding skin layer thickness, skin cell types and distribution, and skin repair mechanisms.

SEM was employed to evaluate *C. auris* biomass dispersion and biofilm structure on the skin. Following *C. auris* introduction, a low-magnification examination revealed fungal growth on the porcine skin surface. At higher magnification, multilayer biofilms containing yeast cells were observed in the control and the 209  $\mu$ M FLZ group. A significant change was not observed in *C. auris* numbers on the porcine skin with 7.4 and 14.8  $\mu$ M BE concentrations compared to the control group. This indicated that the inhibitory effect of *C. auris* on adherence to porcine skin was weak at these concentrations. However, at 29.6 and 59.2  $\mu$ M BE concentrations, the number of *C. auris* on pig skin significantly decreased, showing only a single layer of adherence. The number of *C. auris* adhesions significantly decreased, resulting in a single layer (Fig. 14B). BE also enhanced larval survival. By the end of the 5th day, all larvae infected by *C. auris* had lost their vitality. At concentrations of 7.4, 14.8, and 29.6  $\mu$ M BE and 209  $\mu$ M FLZ, survival rates were 20%, 40%, and 20%, respectively, while 59.2  $\mu$ M BE significantly increased survival to 70% in *C. auris*. (Fig. 15A and B) This indicates that BE enhances the viability of *G. mellonella* larvae.

### RT-qPCR results reveal the mechanisms of BE against *C. auris*

To confirm the transcriptome results, we selected the two most differentially expressed genes (DEGs) from each of the four groups of virulence-related genes for RT-qPCR. *SCF1* and *ALS7* encode adhesins that facilitate *Candida* adhesion. *SNQ2* and *YCF1* are classified as ATP-binding cassette (ABC) transporters, specifically belonging to the group of multiple drug resistance-associated protein-like transporters. *ERG25* and *ERG12* are closely associated with the biosynthesis of ergosterol within the cell membrane. This process is essential for maintaining the integrity and function of the

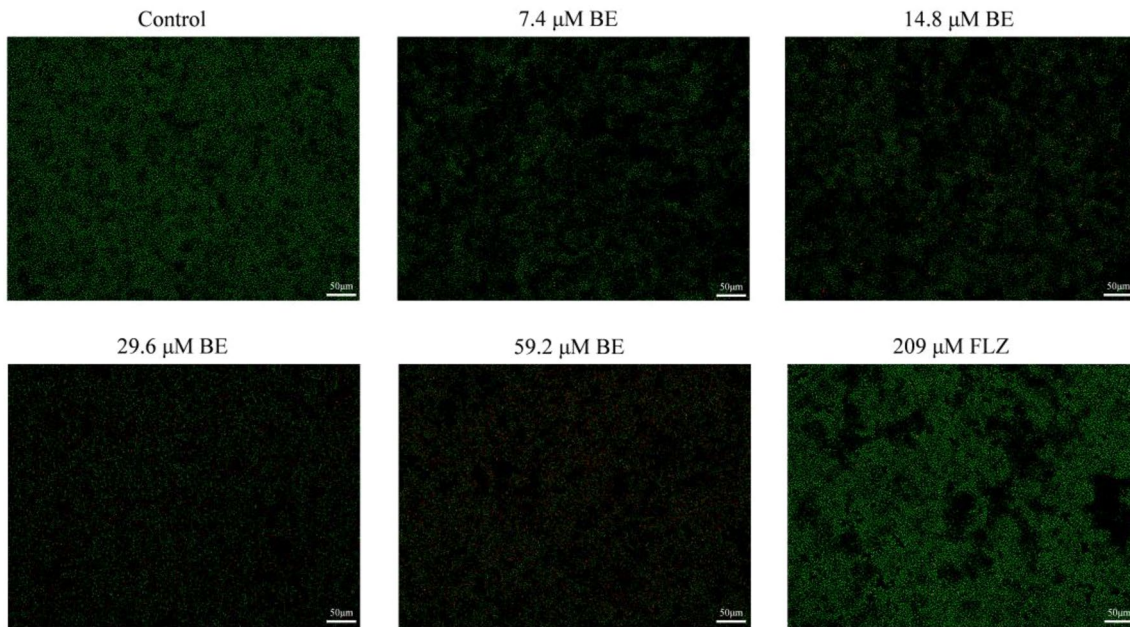


**Fig. 10** Baicalein (BE) promotes the death of *C. auris* biofilm cells. Images represent the survival of *C. auris* in the biofilm state under fluorescence microscopic observation. Scale bars 50  $\mu\text{m}$

cell membrane. *RBT5* and *PGA4* are essential components of the cell wall proteome. The results showed significant downregulation of all genes under BE treatment, consistent with the transcriptome data (Fig. 16). This indicated that BE might affect related mechanisms to inhibit *C. auris*.

## Discussion

Recently, the proportion of non-*C. albicans* infections increase annually. All *Candida* pathogens, including *C. albicans*, cause superficial and systemic infections of varying severity. *C. auris*, also known as the “superbug,” emerges as a rapidly growing pathogen. Its rapid global spread over the last decade has triggered several hospital-acquired infection outbreaks (Ruiz-Gaitán et al. 2018), posing a significant threat to human health. *C. auris* infects patients of all ages, causing invasive infections (Du et al. 2020), including bloodstream infections in patients in intensive care units. It colonizes various human body parts, such as the skin, respiratory tract, and urinary tract. Its survival time in the environment is prolonged, making it difficult to remove. Consequently, using equipment such as implanted catheters and invasive medical instruments often results in cross-infection with *C. auris* (Biswal et al. 2017).

Additionally, the most prominent feature of *C. auris* is drug resistance or multidrug resistance, leading to treatment failure and challenges in epidemic control. In 2019, the Centers for Disease Control and Prevention (CDC) categorized

pathogenic microorganisms into four threat levels in the antibiotic resistance threats report: urgent, serious, containing, and watch list threats. *C. auris* was classified as an urgent threat, emphasizing the importance of studying its drug resistance and mechanisms. The CDC has reported a series of drug patterns against *C. auris* by monitoring MIC data for commonly used antifungal drugs over the past decade. Specifically, 90% of *C. auris* strains showed high resistance to fluconazole, with a drug breakpoint of  $\text{MIC} \geq 104.5 \mu\text{M}$ , 30% of the strains were resistant to the polyene drug amphotericin B, with a drug breakpoint of  $\text{MIC} \geq 2.2 \mu\text{M}$ . A small minority of strains (<5%) were resistant to the echinocandin drug caspofungin, with a drug breakpoint of  $\text{MIC} \geq 1.8 \mu\text{M}$  (Chaabane et al. 2019). In our research, we discovered that the MIC of BE against *C. auris* ranged from 0.93–1.85  $\mu\text{M}$ , indicating its potent growth inhibition activity against *C. auris*. Compared to the three common antifungal drugs mentioned above, BE demonstrated even greater effectiveness in inhibiting *C. auris*. Considering the toxicity and high cost associated with currently used antifungal agents, BE shows promising potential for the treatment of *C. auris* infection.

To understand the molecular interactions between BE and *C. auris*, we conducted a comparative analysis of the gene expression profiles of BE-treated *C. auris* cells (59.2  $\mu\text{M}$ ) with untreated cells. Our findings reveal significant changes in the expression levels of 4,062 genes in the BE-treated group compared to those of the untreated control group. We specifically examined differentially expressed genes distinct to the BE-treated group and found downregulation of several



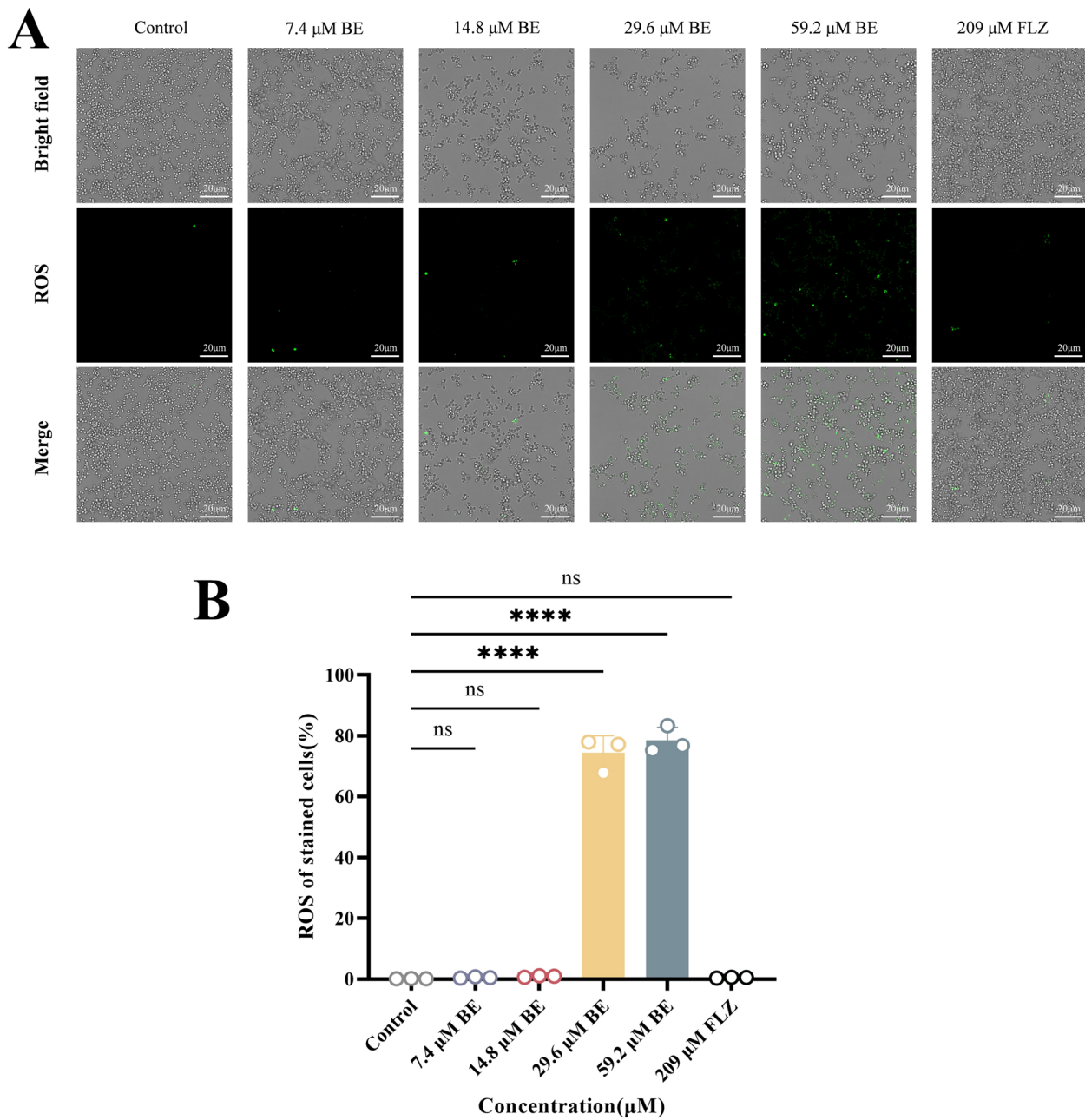


**Fig. 11** The impact of baicalein (BE) on the generation of reactive oxygen species (ROS). **A** Images represent the accumulation of ROS, with green fluorescence observed. Scale bars 20 μm. **B** Histogram

displays the proportion of cells that are positive for ROS. All data are presented as mean ±SD: ns = not significant, \*\*\*\**P* < 0.0001 vs. Control group

genes associated with adhesion, biofilm formation, and other virulence factors in the presence of BE. This suggests that BE inhibits *C. auris* through multiple mechanisms.

*C. auris* enhances a significant virulence factor: its exceptional adhesion capability. This underscores the crucial need for early intervention during the early adhesion phase to control fungal infection effectively. Adhesion is facilitated by genes expressing adhesins, among which is the Surface Colonization Factor (*SCF1*), a distinct and

prominent adhesion binding to various surfaces through cation-dependent interactions (Santana et al. 2023). The *ALS* (agglutinin-like sequence) gene family encodes proteins that facilitate the adherence of the yeast *Candida albicans* to endothelial and epithelial cells. *ALS7* is a hypermutable contingency locus and plays a crucial role in the pathogenicity of *Candida* as an opportunistic human pathogen (Zhang et al. 2003). Flocculation is also closely associated with adhesin expression (Gelís et al. 2012). Our RT-qPCR



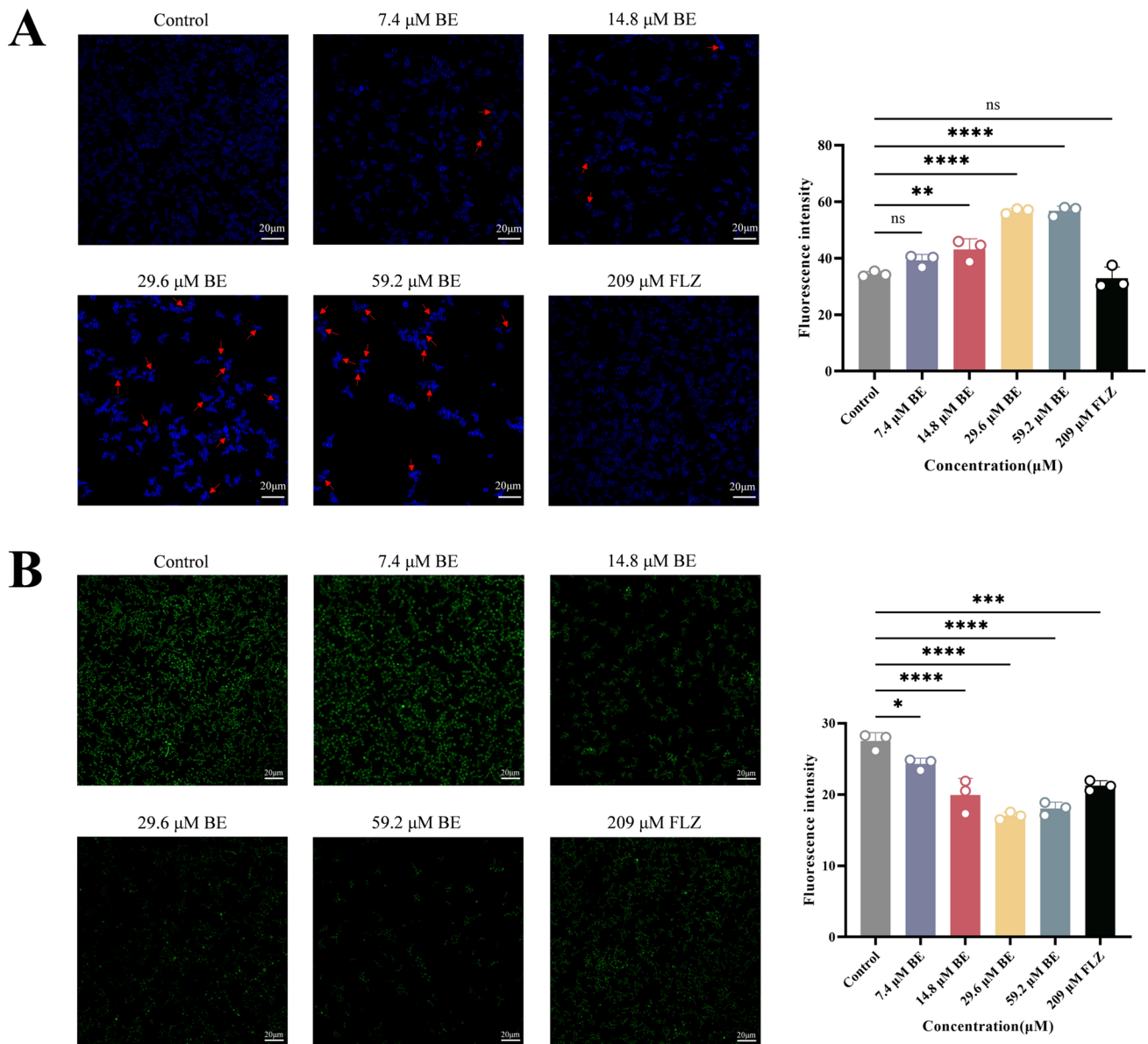


**Fig. 12** The effect of baicalein (BE) on the *C. auris* cell wall. **A** Images represent *C. auris* with or without BE treatment was stained with calcofluor white (CFW). The deposition of chitin is indicated by red arrows. Scale bars 20 μm. The fluorescence intensity of CFW-stained cells was used to measure the levels of chitin. **B** Images rep-

resent *C. auris* with or without BE treatment was stained with aniline blue. Scale bars 20 μm. The levels of glucan were quantified through the fluorescence intensity of cells stained with aniline blue. All data are presented as mean ± SD: ns = not significant, \* $P < 0.05$ , \*\* $P < 0.01$ , \*\*\* $P < 0.001$ , \*\*\*\* $P < 0.0001$  vs. Control group

findings revealed a significant reduction in the expression levels of *SCF1* and *ALS7* after BE treatment. Furthermore, BE significantly inhibited flocculation and CSH in *C. auris*, reducing its adherence to cells. The FLZ treatment, however, did not yield satisfactory results as it showed minimal inhibitory effect on the adhesion of *C. auris*. These findings suggest that targeting adhesion-related genes to disrupt the initial adhesion stages could be an effective treatment for treating *C. auris* infection.

Biofilm formation becomes a crucial factor in *C. auris* virulence as adhesion progresses. Biofilms exhibit higher resistance to antifungal agents than that of the planktonic cells. A previous study found that the MBEC of antifungals against biofilms significantly surpassed the MIC values against planktonic cells (Oyardi et al. 2023). Our study also revealed that SMIC values against biofilms were significantly higher than those of the MIC against planktonic cells. The XTT and crystal violet assays indicated that BE treatment suppressed the metabolic activity and biomass of

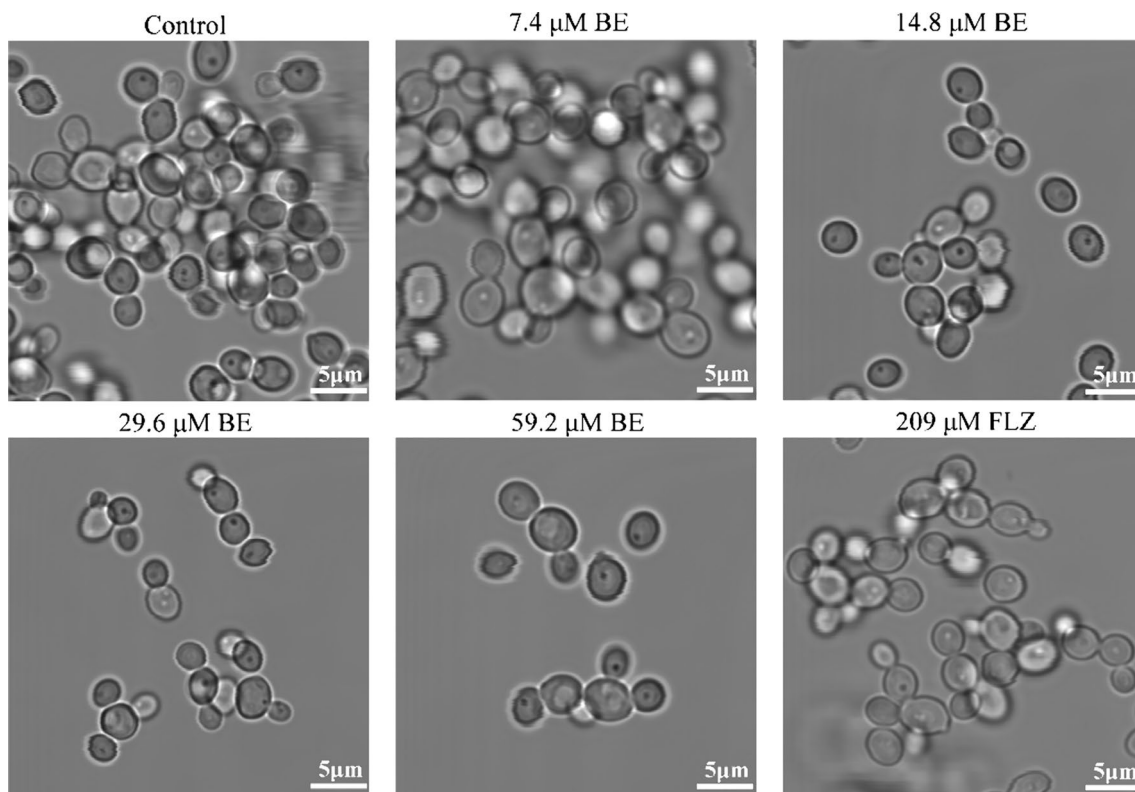


**Fig. 13** Baicalein (BE) inhibits the aggregation of *C. auris*. Images represent the aggregation of *C. auris* following treatment with BE. Scale bars 5  $\mu\text{m}$

*C. auris* biofilms, while FLZ treatment exhibited minimal inhibitory effect. CLSM and SEM images revealed densely packed/oval cells in *C. auris* biofilms. Furthermore, BE treatment resulted in a concentration-dependent decrease in biomass and cell density of *C. auris* biofilms, while FLZ treatment did not exhibit inhibitory effects on biofilm formation.

Efflux pump expression is responsible for antimicrobial resistance within biofilm structures. In fungi, some pump proteins facilitate the transport of intracellular antifungal drugs to the extracellular milieu, leading to reduced drug concentrations within cells and subsequently reducing drug efficacy (Jangir et al. 2023). R6G was employed to measure intracellular fluorescence intensity after drug administration to *C. auris*, investigating whether the inhibitory effect of BE on *Candida auriculata* was related to drug efflux. Flow cytometry results showed that BE reduced biofilm resistance by affecting efflux pump expression. In contrast, the FLZ did not affect the expression of efflux pumps. *SNQ2* and *YCF1* are categorized as multiple drug resistance-associated protein-like transporters—ATP-binding cassette (ABC) transporters. Yeast survives in micro environments utilizing ABC transporters to circumvent toxins and a variety of drugs (Buechel and Pinkett 2020). Consistent with our RT-qPCR

results, *SNQ2* and *YCF1* expression levels significantly decreased after BE intervention.

*Candida* spp. secrete hydrolytic enzymes, such as proteinases, phospholipases, esterase, and hemolysins, crucial for causing disease. These enzymes assist in binding to host tissues and damaging the host cell membrane. Phospholipases target cell membrane phospholipids, while esterase degrade ester bonds. Hemolysin enhances virulence by breaking down hemoglobin for iron extraction. These enzymes enable *Candida* spp. To infiltrate mucous membranes and blood vessels while evading host immune detection. A previous study found that various strains exhibited diverse virulence factors; however, all strains displayed proteinase activity. Additionally, 67.3% of these strains showed phospholipase activity, and 68.2% exhibited hemolysin activity (Larkin et al. 2017). Another study showed that 96% of strains exhibited proteinase activity, while none showed phospholipase activity (Shaban et al. 2020). Our study revealed no proteinase or hemolysin activity in any isolates. However, all isolates exhibited weak phospholipase and esterase activities. Among them, BE weakly inhibited the secretion of phospholipase and esterase, while FLZ did not exhibit any inhibitory effect. This suggests that *C. auris* may exhibit strain-dependent phenotypes that affect its pathogenicity. Various studies

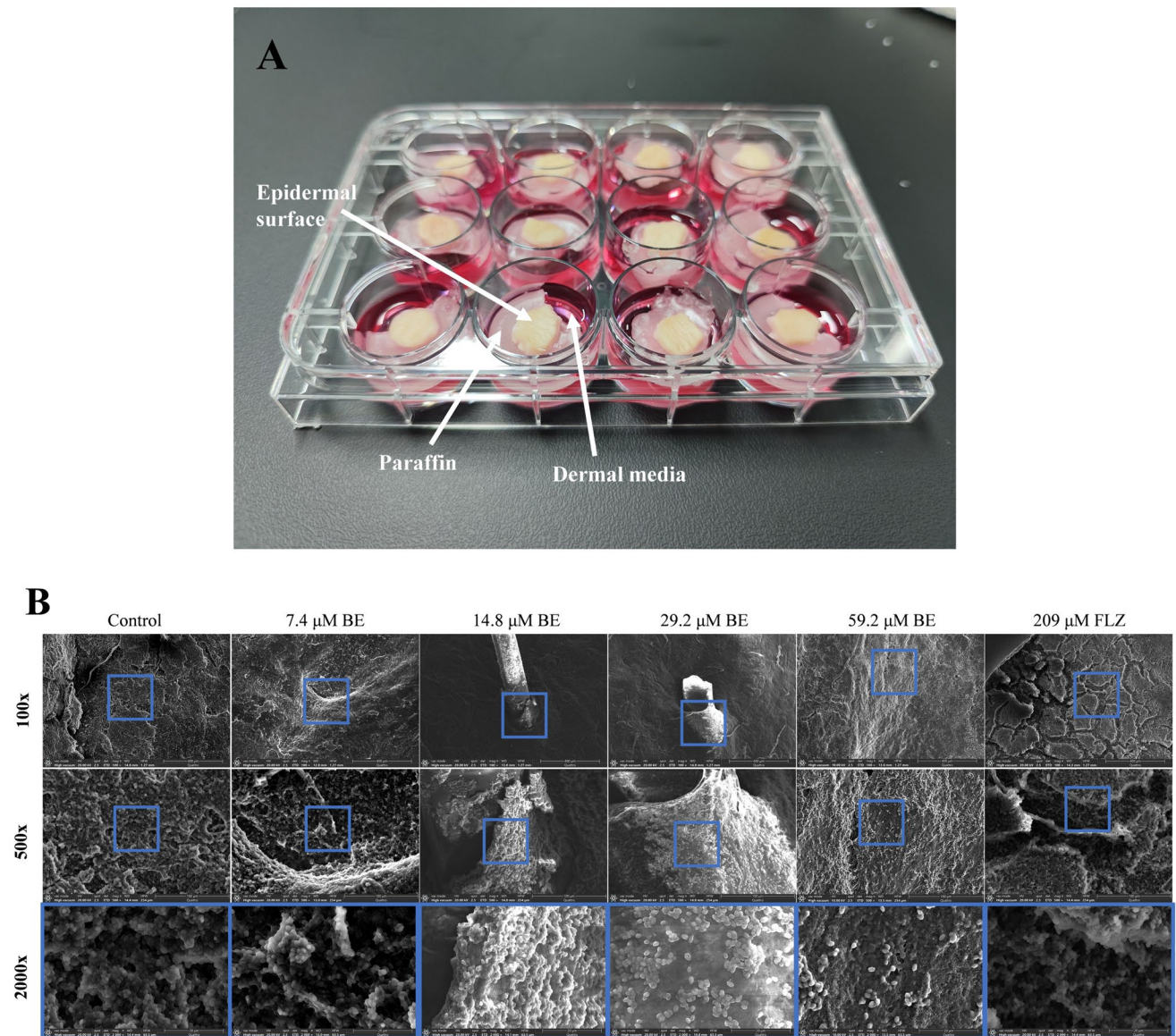


**Fig. 14** Baicalein (BE) inhibit the adhesion of *C. auris* to porcine skin. **A** The porcine skin samples were immersed in Dulbecco's modified Eagle's medium (DMEM) with 10% Fetal Bovine Serum (FBS), and the paraffin method was used to separate the epidermal surface

from the liquid medium. **B** *C. auris* biofilms were cultured on samples of porcine skin and observed using scanning electron microscope (SEM)

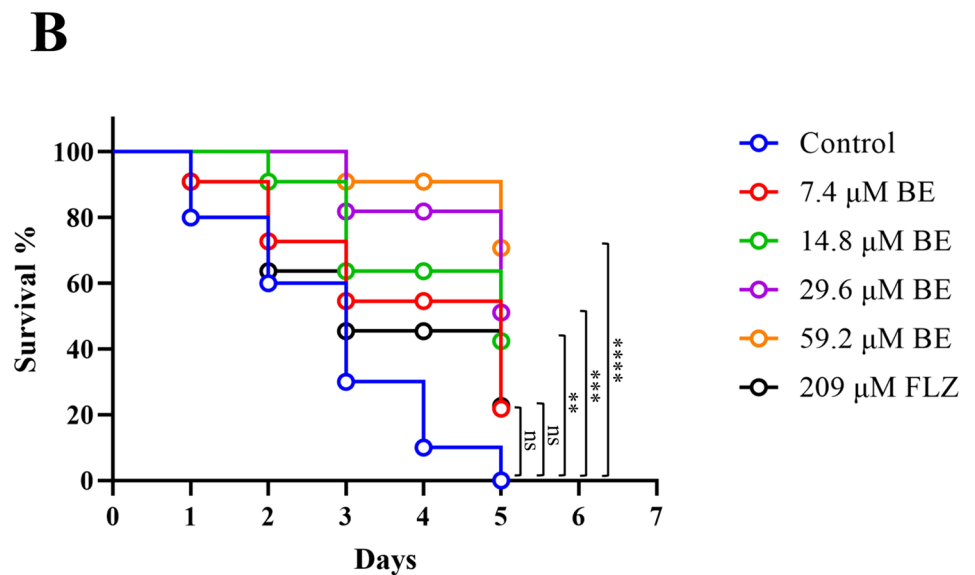
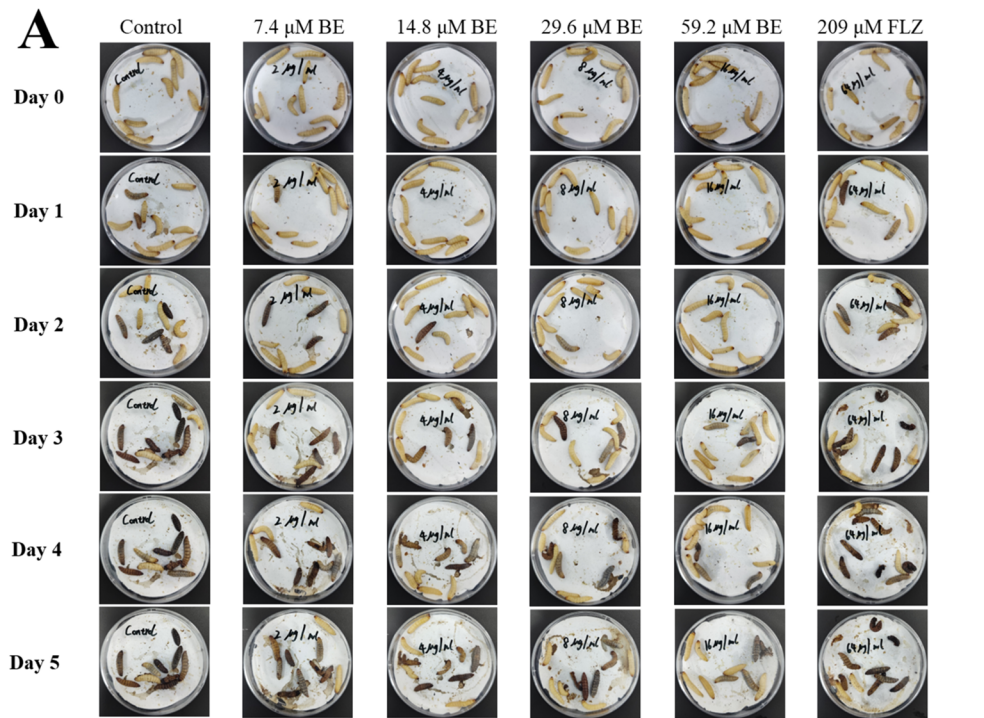
have observed variations in virulence traits among *C. auris* strains, which can be attributed to the distinct characteristics of isolates from different geographical clades (Oyardi et al. 2023).

The cell membrane plays a vital role in normal growth, reproduction, and metabolism of fungal cells. In our investigation into the effect of BE on *C. auris* structure, we evaluated cell membrane integrity using PI, a fluorescent dye that penetrates cells through damaged membranes and binds to nucleic acids, causing red fluorescence. These findings revealed a significant increase in red cells post-BE treatment, while the FLZ treatment had no red cells. After BE

intervention, our RT-qPCR results also showed reduced expression levels of *ERG25* and *ERG12*, genes closely linked to ergosterol biosynthesis within the cell membrane. One of the essential membrane lipids is sterols, among which ergosterol is the most abundant in fungal cells and mainly resides in the plasma membrane. Meanwhile, ergosterol biosynthesis is one of the major targets of antifungal therapies (Jordá et al. 2023). Above findings have confirmed that BE has the capability to disrupt the cell membrane of *C. auris* and impact the formation of the cell membrane. ROS typically function as signaling molecules in normal physiological and fungal growth processes. However, excessive



**Fig. 15** Baicalein (BE) therapy influenced larval survival. **A** Images represent larvae ( $n = 10$ ) infected by *C. auris* after treatment with BE. **B** The Kaplan–Meier method and log rank test were utilized to analyze survival curves and identify differences. All data are presented as mean  $\pm$  SD: ns = not significant, \*\* $P < 0.01$ , \*\*\* $P < 0.001$ , \*\*\*\* $P < 0.0001$  vs. Control group



ROS can cause cell death or pathological alterations due to their damaging effects. Our study reveals that BE disrupts membrane integrity, leading to ROS accumulation, suggesting the potential of BE to induce apoptosis in *C. auris*. However, FLZ did not have any effect on *C. auris* apoptosis.

The fungal cell wall, comprising mannoprotein,  $\beta$ -glucan, and chitin, is essential for maintaining cell shape and protecting against external factors (Hasim and Coleman 2019). The inner chitin/glucan layer plays a crucial role in preserving

cell morphology and providing structural stability. Our study reveals that BE induces cell wall destabilization, leading to increased chitin deposition and reduced glucan expression, while FLZ had little impact on the cell wall. After BE intervention, our RT-qPCR results also showed downregulated expression levels of *RBT5* and *PGA4*, integral parts of the cell wall proteome. *PGA4* is a 1,3- $\beta$ -glucan transferase responsible for elongating the 1,3- $\beta$ -glucan chain in the cell wall and playing a crucial role in cell wall biosynthesis and

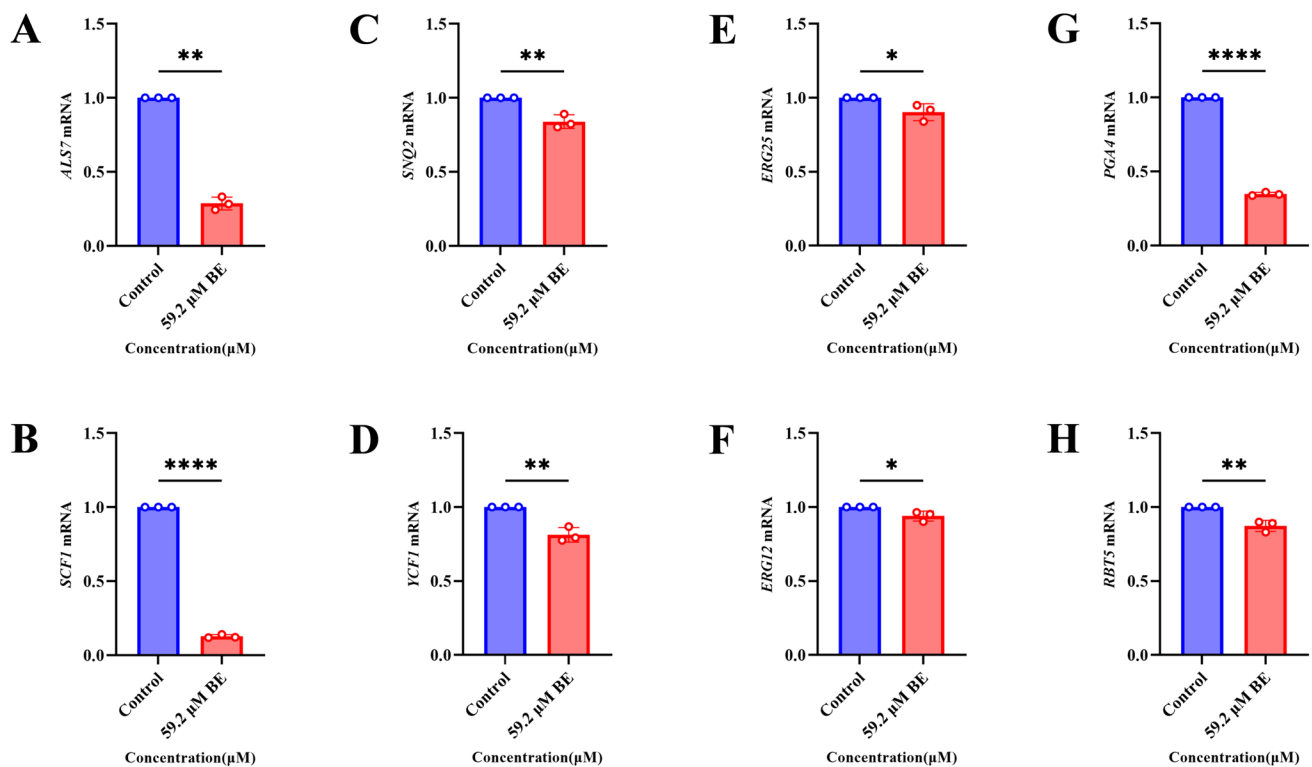


**Fig. 16** Baicalein (BE) inhibits *C. auris* through potential mechanisms (A-H) RT-qPCR were used to detect expression of *ALS7*, *SCF1*, *SNQ2*, *YCF1*, *ERG25*, *ERG12*, *RBT5*, *PGA4* mRNA. All data are presented as mean  $\pm$  SD: \* $P < 0.05$ , \*\* $P < 0.01$ , \*\*\*\* $P < 0.0001$  vs. Control group

morphogenesis (Plaine et al. 2008). *RBT5* is an extracellular glycosylphosphatidylinositol (GPI)-anchored heme-binding protein, which plays a crucial role in facilitating heme-iron uptake and forming a cross-cell wall heme-transfer cascade (Kuznets et al. 2014). Additionally, cell wall proteins could potentially enhance the aggregative phenotype of *C. auris* and its adaptability, potentially affecting its persistence and virulence (Wang et al., 2024). Our findings suggest that BE inhibits the aggregation of *C. auris*, and FLZ also exhibits some inhibitory effects.

*Candida* colonization is a crucial step in the development of invasive candidiasis. Results from the porcine skin model showed that *C. auris* could grow and survive on skin surfaces and in environments with skin components, forming dense biofilms on porcine skin. This explains its tendency to colonize the skin, endure on hospital surfaces, and spread efficiently in healthcare settings. Similarly, we observed that BE effectively inhibited *C. auris* colonization of porcine skin, while FLZ did not show the same effectiveness. The *G. mellonella* larval model effectively exhibited the potential of BE to inhibit the invasion of organisms by *C. auris*, whereas FLZ also did not exhibit similar effects.

## Conclusions

In conclusion, this study suggests that BE could serve as a novel antifungal and anti-biofilm agent. We showed its efficacy in inhibiting multidrug-resistant *C. auris* through in vitro phenotypic and genotypic analyses. However, further in vivo studies are necessary to elucidate the mechanisms of action of BE against *C. auris* and evaluate its potential clinical applications in the pharmaceutical industry.

**Acknowledgements** This work was supported by the National Natural Science Foundation of China (Grant Nos. 82374173, 81774034, 81573725), and the Key Research and Development Projects of Anhui Province (202104a07020020), the Key scientific research projects of Anhui Provincial Department of Education (KJ2021A0590), the National College Students' innovation and entrepreneurship training program (S202310369139)

**Author contributions** All the authors contributed extensively to the work presented in this manuscript. The study was conceived by LC and WCZ. Experimental procedures were carried out by LC, WH. Data analyses were performed by LC, WJ, WYM, LH, WH, WWF, WDO, SJ, WTM. The paper was written by LC, WCZ.

**Funding** National Natural Science Foundation of China, Changzhong Wang, 82374173, 81774034.

**Data availability** No datasets were generated or analysed during the current study.



## Declarations

**Conflict of interests** The authors declare that they have no known competing financial interests or personal relationships that could have appeared to influence the work reported in this paper.

## References

- Ahmad S, Khan Z, Al-Sweih N, Alfouzan W, Joseph L (2020) *Candida auris* in various hospitals across Kuwait and their susceptibility and molecular basis of resistance to antifungal drugs. *Mycoses* 63(1):104–112. <https://doi.org/10.1111/myc.13022>
- Ben Abid F, Salah H, Sundararaju S, Dalil L, Abdelwahab AH, Salameh S, Ibrahim EB, Almaslmani MA, Tang P, Perez-Lopez A, Tsui CKM (2023) Molecular characterization of *Candida auris* outbreak isolates in Qatar from patients with COVID-19 reveals the emergence of isolates resistant to three classes of antifungal drugs. *Clin Microbiol Infect* 29(8):1083.e1–1083.e7. <https://doi.org/10.1016/j.cmi.2023.04.025>
- Bing J, Guan Z, Zheng T, Ennis CL, Nobile CJ, Chen C, Chu H, Huang G (2024) Rapid evolution of an adaptive multicellular morphology of *Candida auris* during systemic infection. *Nat Commun* 15(1):2381. <https://doi.org/10.1038/s41467-024-46786-8>
- Biswal M, Rudramurthy SM, Jain N, Shamanth AS, Sharma D, Jain K, Yaddanapudi LN, Chakrabarti A (2017) Controlling a possible outbreak of *Candida auris* infection: lessons learnt from multiple interventions. *J Hosp Infect* 97(4):363–370. <https://doi.org/10.1016/j.jhin.2017.09.009>
- Buechel ER, Pinkett HW (2020) Transcription factors and ABC transporters: from pleiotropic drug resistance to cellular signaling in yeast. *FEBS Lett* 594(23):3943–3964. <https://doi.org/10.1002/1873-3468.13964>
- Chaabane F, Graf A, Jequier L, Coste AT (2019) Review on Antifungal Resistance Mechanisms in the Emerging Pathogen *Candida auris*. *Front Microbiol* 10:2788. <https://doi.org/10.3389/fmicb.2019.02788>
- Chow NA, de Groot T, Badali H, Abastabar M, Chiller TM, Meis JF (2019) Potential Fifth Clade of *Candida auris*, Iran, 2018. *Emerg Infect Dis* 25(9):1780–1781. <https://doi.org/10.3201/eid2509.190686>
- Dai BD, Cao YY, Huang S, Xu YG, Gao PH, Wang Y, Jiang YY (2009) Baicalein induces programmed cell death in *Candida albicans*. *J Microbiol Biotechnol* 19(8):803–809
- Du H, Bing J, Hu T, Ennis CL, Nobile CJ, Huang G (2020) *Candida auris*: Epidemiology, biology, antifungal resistance, and virulence. *PLoS Pathog* 16(10):e1008921. <https://doi.org/10.1371/journal.ppat.1008921>
- Gelis S, de Groot PW, Castillo L, Moragues MD, Sentandreu R, Gómez MM, Valentín E (2012) Pga13 in *Candida albicans* is localized in the cell wall and influences cell surface properties, morphogenesis and virulence. *Fungal Genet Biol* 49(4):322–331. <https://doi.org/10.1016/j.fgb.2012.01.010>
- Hasim S, Coleman JJ (2019) Targeting the fungal cell wall: current therapies and implications for development of alternative antifungal agents. *Future Med Chem* 11(8):869–883. <https://doi.org/10.4155/fmc-2018-0465>
- Horton MV, Johnson CJ, Kernien JF, Patel TD, Lam BC, Cheong JZA, Meudt JJ, Shanmuganayagam D, Kalan LR, Nett JE (2020) *Candida auris* Forms High Burden Biofilms in Skin Niche Conditions and on Porcine Skin. *mSphere*. 5(1):00910. <https://doi.org/10.1128/mSphere.00910-19>
- Hu K, Zhang H, Shi G, Wang B, Wu D, Shao J, Wang T, Wang C (2023) Effects of n-butanol extract of Pulsatilla decoction on the NLRP3 inflammasome in macrophages infected with *Candida albicans*. *J Ethnopharmacol* 304:116041. <https://doi.org/10.1016/j.jep.2022.116041>
- Jakab Á, Kovács F, Balla N, Nagy-Köteles C, Ragyák Á, Nagy F, Borman AM, Majoros L, Kovács R (2024) Comparative transcriptional analysis of *Candida auris* biofilms following farnesol and tyrosol treatment. *Microbiol Spectr* 12(4):e0227823. <https://doi.org/10.1128/spectrum.02278-23>
- Janecko M, Gmur D, Kochanowicz E, Górka K, Skrzypek T (2022) Inhibitory effect of a combination of baicalein and quercetin flavonoids against *Candida albicans* strains isolated from the female reproductive system. *Fungal Biol* 126(6–7):407–420. <https://doi.org/10.1016/j.funbio.2022.05.002>
- Jangir P, Kalra S, Tanwar S, Bari VK (2023) Azole resistance in *Candida auris*: mechanisms and combinatorial therapy. *APMIS* 131(8):442–462. <https://doi.org/10.1111/apm.13336>
- Jordá T, Rozès N, Martínez-Pastor MT, Puig S (2023) The yeast mRNA-binding protein Cth2 post-transcriptionally modulates ergosterol biosynthesis in response to iron deficiency. *Biochim Biophys Acta Gene Regul Mech* 1866(3):194959. <https://doi.org/10.1016/j.bbagr.2023.194959>
- Kumar D, Banerjee T, Pratap CB, Tilak R (2015) Itraconazole-resistant *Candida auris* with phospholipase, proteinase and hemolysin activity from a case of vulvovaginitis. *J Infect Dev Ctries* 9(4):435–437. <https://doi.org/10.3855/jidc.4582>
- Kuznetsk G, Vigonsky E, Weissman Z, Lalli D, Gildor T, Kauffman SJ, Turano P, Becker J, Lewinson O, Kornitzer D (2014) A relay network of extracellular heme-binding proteins drives *C. albicans* iron acquisition from hemoglobin. *PLoS Pathog* 10(10):e1004407. <https://doi.org/10.1371/journal.ppat.1004407>
- Larkin E, Hager C, Chandra J, Mukherjee PK, Retuerto M, Salem I, Long L, Isham N, Kovanda L, Borroto-Esoda K, Wring S, Angulo D, Ghannoum M (2017) The Emerging Pathogen *Candida auris*: Growth Phenotype, Virulence Factors, Activity of Antifungals, and Effect of SCY-078, a Novel Glucan Synthesis Inhibitor, on Growth Morphology and Biofilm Formation. *Antimicrob Agents Chemother* 61(5):e02396-e2416. <https://doi.org/10.1128/AAC.02396-16>
- Lei J, Huang J, Xin C, Liu F, Zhang J, Xie Y, Mao Y, Chen W, Song Z (2023) Riboflavin Targets the Cellular Metabolic and Ribosomal Pathways of *Candida albicans* In Vitro and Exhibits Efficacy against Oropharyngeal Candidiasis. *Microbiol Spectr* 11(1):e0380122. <https://doi.org/10.1128/spectrum.03801-22>
- Li-Weber M (2009) New therapeutic aspects of flavones: the anticancer properties of Scutellaria and its main active constituents Wogonin, Baicalein and Baicalin. *Cancer Treat Rev* 35(1):57–68. <https://doi.org/10.1016/j.ctrv.2008.09.005>
- Malavia-Jones D, Farrer RA, Stappers MHT, Edmondson MB, Borman AM, Johnson EM, Lipke PN, Gow NAR (2023) Strain and temperature dependent aggregation of *Candida auris* is attenuated by inhibition of surface amyloid proteins. *Cell Surf* 10:100110. <https://doi.org/10.1016/j.tcs.2023.100110>
- Nandhagopal M, Mala R, Somarathinam K, Dhakshinamurthy D, Narayanasamy M, Vijayan P, Shankar MM (2024) Anti-fungal effects of novel N-(tert-butyl)-2-(pyridin-2-yl)imidazo[1,2-a]pyridin-3-amine derivative and its in-vitro, in-silico, and mode of action against *Candida* spp. *Arch Microbiol* 206(4):186. <https://doi.org/10.1007/s00203-023-03780-w>
- Oyardi O, Demir ES, Alkan B, Komec S, Genc GE, Aygun G, Teke L, Turan D, Erturan Z, Savage PB, Guzel CB (2023) Phenotypic Investigation of Virulence Factors, Susceptibility to Ceragenins, and the Impact of Biofilm Formation on Drug Efficacy in *Candida auris* Isolates from Türkiye. *J Fungi (basel)* 9(10):1026. <https://doi.org/10.3390/jof9101026>
- Pan M, Wang Q, Cheng T, Wu D, Wang T, Yan G, Shao J (2021) Paeonol assists fluconazole and amphotericin B to inhibit virulence

- factors and pathogenicity of *Candida albicans*. Biofouling 37(8):922–937. <https://doi.org/10.1080/08927014.2021.1985473>
- Plaine A, Walker L, Da Costa G, Mora-Montes HM, McKinnon A, Gow NA, Gaillardin C, Munro CA, Richard ML (2008) Functional analysis of *Candida albicans* GPI-anchored proteins: roles in cell wall integrity and caspofungin sensitivity. Fungal Genet Biol 45(10):1404–1414. <https://doi.org/10.1016/j.fgb.2008.08.003>
- Ramos LS, Parra-Giraldo CM, Branquinha MH, Santos ALS (2023) Cell Aggregation Capability of Clinical Isolates from *Candida auris* and *Candida haemulonii* Species Complex. Trop Med Infect Dis 8(8):382. <https://doi.org/10.3390/tropicalmed8080382>
- Ruiz-Gaitán A, Moret AM, Tasiás-Pitarch M, Aleixandre-López AI, Martínez-Morel H, Calabuig E, Salavert-Lletí M, Ramírez P, López-Hontangas JL, Hagen F, Meis JF, Mollar-Maseres J, Pemán J (2018) An outbreak due to *Candida auris* with prolonged colonisation and candidaemia in a tertiary care European hospital. Mycoses 61(7):498–505. <https://doi.org/10.1111/myc.12781>
- Santana DJ, Anku JAE, Zhao G, Zarnowski R, Johnson CJ, Hautau H, Visser ND, Ibrahim AS, Andes D, Nett JE, Singh S, O'Meara TR (2023) A *Candida auris*-specific adhesin, Scf1, governs surface association, colonization, and virulence. Science 381(6665):1461–1467. <https://doi.org/10.1126/science.adf8972>
- Satoh K, Makimura K, Hasumi Y, Nishiyama Y, Uchida K, Yamaguchi H (2009) *Candida auris* sp Nov, a novel ascomycetous yeast isolated from the external ear canal of an inpatient in a Japanese hospital. Microbiol Immunol 53(1):41–44. <https://doi.org/10.1111/j.1348-0421.2008.00083.x>
- Shaban S, Patel M, Ahmad A (2020) Improved efficacy of antifungal drugs in combination with monoterpene phenols against *Candida auris*. Sci Rep 10(1):1162. <https://doi.org/10.1038/s41598-020-58203-3>
- Shirley KP, Windsor LJ, Eckert GJ, Gregory RL (2017) In Vitro Effects of Plantago Major Extract, Aucubin, and Baicalein on *Candida albicans* Biofilm Formation, Metabolic Activity, and Cell Surface Hydrophobicity. J Prosthodont 26(6):508–515. <https://doi.org/10.1111/jopr.12411>
- Sun C, Zhao X, Jiao Z, Peng J, Zhou L, Yang L, Huang M, Tian C, Guo G (2022) The Antimicrobial Peptide AMP-17 Derived from *Musca domestica* Inhibits Biofilm Formation and Eradicates Mature Biofilm in *Candida albicans*. Antibiotics (basel) 11(11):1474. <https://doi.org/10.3390/antibiotics11111474>
- Vélez N, Argel A, Kissmann AK, Alpízar-Pedraza D, Escandón P, Rosenau F, Ständker L, Firacative C (2024) Pore-forming peptide C14R exhibits potent antifungal activity against clinical isolates of *Candida albicans* and *Candida auris*. Front Cell Infect Microbiol 14:1389020. <https://doi.org/10.3389/fcimb.2024.1389020>
- Wei PW, Wang X, Wang C, Chen M, Liu MZ, Liu WX, He YL, Xu GB, Zheng XH, Zhang H, Liu HM, Wang B (2024) Ginkgo biloba L exocarp petroleum ether extract inhibits methicillin-resistant *Staphylococcus aureus* by modulating ion transport, virulence, and biofilm formation in vitro and in vivo. J Ethnopharmacol 328:117957. <https://doi.org/10.1016/j.jep.2024.117957>
- Wu R, Murali R, Kabe Y, French SW, Chiang YM, Liu S, Sher L, Wang CC, Louie S, Tsukamoto H (2018) Baicalein Targets GTPase-Mediated Autophagy to Eliminate Liver Tumor-Initiating Stem Cell-Like Cells Resistant to mTORC1 Inhibition. Hepatology 68(5):1726–1740. <https://doi.org/10.1002/hep.30071>
- Wu Y, Chen Y, Lu H, Ying C (2023) Miltefosine exhibits fungicidal activity through oxidative stress generation and Aif1 activation in *Candida albicans*. Int J Antimicrob Agents 62(1):106819. <https://doi.org/10.1016/j.ijantimicag.2023.106819>
- Wu H, Li C, Wang Y, Zhang M, Wu D, Shao J, Wang T, Wang C (2024) Transcriptomics Reveals Effect of Pulsatilla Decoction Butanol Extract in Alleviating Vulvovaginal Candidiasis by Inhibiting Neutrophil Chemotaxis and Activation via TLR4 Signaling. Pharmaceuticals (basel, Switzerland) 17(5):594. <https://doi.org/10.3390/ph17050594>
- Yan JJ, Du GH, Qin XM, Gao L (2020) Baicalein attenuates the neuro-inflammation in LPS-activated BV-2 microglial cells through suppression of pro-inflammatory cytokines, COX2/NF- $\kappa$ B expressions and regulation of metabolic abnormality. Int Immunopharmacol 79:106092. <https://doi.org/10.1016/j.intimp.2019.106092>
- Zhang N, Harrex AL, Holland BR, Fenton LE, Cannon RD, Schmid J (2003) Sixty alleles of the ALS7 open reading frame in *Candida albicans*: ALS7 is a hypermutable contingency locus. Genome Res 13(9):2005–2017. <https://doi.org/10.1101/gr.1024903>
- Zhang MX, Xia D, Shi GX, Shao J, Wang TM, Tang CC, Wang CZ (2015) Inhibitory effects of butyl alcohol extract of Baitouweng decoction on yeast-to-hyphae transition of *Candida albicans* isolates from VVC in alkaline pH environment. China J Chin Materia Medica 40(4):710–715
- Zhang J, Jiang X, Shi G, Zhang H, Hu K, Wu D, Shao J, Liu T, Wang T, Wang C (2024) Effect of the Pulsatilla decoction n-butanol extract on vulvovaginal candidiasis caused by *Candida glabrata* and on its virulence factors. Fitoterapia 173:105825. <https://doi.org/10.1016/j.fitote.2024.105825>

**Publisher's Note** Springer Nature remains neutral with regard to jurisdictional claims in published maps and institutional affiliations.

Springer Nature or its licensor (e.g. a society or other partner) holds exclusive rights to this article under a publishing agreement with the author(s) or other rightsholder(s); author self-archiving of the accepted manuscript version of this article is solely governed by the terms of such publishing agreement and applicable law.